Talanta

Single virus inductively coupled plasma mass spectroscopy analysis: a comprehensive study.

--Manuscript Draft--

Manuscript Number:	TAL-D-20-04702R2
Article Type:	Research Paper
Section/Category:	Atomic Spectroscopy
Keywords:	Virus identification; virus counting; SP ICP-MS; individual virus analysis; single virus ICP-MS
Corresponding Author:	Claude Degueldre, Dr Lancaster University Lancaster, UNITED KINGDOM
First Author:	Claude Degueldre, Dr
Order of Authors:	Claude Degueldre, Dr
Abstract:	The characterisation of individual nanoparticles by single particle ICP-MS (SP-ICP-MS) has paved the way for the analysis of smallest biological systems. This study suggests to adapting this method for single viruses (SV) identification and counting. With multi-channel ICP-MS records in SV detection mode, the counting of master and key ions can allow analysis and identification of single viruses. The counting of 2-500 virial units can be performed in 20 s. Analyses are proposed to be carried out in Ar torch for master ions: $^{12}C^+$, $^{13}C^+$, $^{14}N^+$, $^{15}N^+$, $^{16}O^+$, $^{18}O^+$ and key ions $^{31}P^+$, $^{32}S^+$, $^{33}S^+$, $^{34}S^+$, $^{76}Se^+$, $^{78}Se^+$, $^{80}Se^+$ and $^{82}Se^+$. All interferences are discussed in detail. The use of MC HR ICP-MS is emphasised while options with dry aerosol and anaerobic/aerobic atmospheres are explored to upgrade the analysis when using quadrupole ICP-MS. Application for two virus types (SARS-COV2 and T5 sipho bacteriophage) is investigated using time scan and fixed mass analysis for the selected virus ions allowing characterisation of the species using the N/C, P/C and S/C molar ratio's and quantification of their number concentration.

Powered by Editorial Manager® and ProduXion Manager® from Aries Systems Corporation

SV ICPMS reply to reviewers
TAL-D-20-04072

In red the last reviewed point from Editor remarks
Thanks for the constructive reviews

Editor
Graphical abstract is new (no gray BG)
References have been completed (doi)
Introduction was revised
Fig 3 updated Ref (also ref cited in Fig 4)
All virus family names in italic
All references were reformatted, specified (full doi) and numbers were checked .
All bold written word/text were reformatted in regular.
Fig. 3: the former virus scheme was replaced by a virus TEM micrograph (similar magnification as Fig 4) and reference given.. Note this image is from the CDC.gov library, free of use for publication.

Reviewer 1-

The viruses are analysed for the following elements:
HCNOPS…
For practical reasons (Ar high purity, and hydration fraction of viruses, residual water injected in plasma) the study does not consider H and O.
Thus the investigation concentrates as on CNPS
In this first study and since data on Se are not reported in the open literature, we eliminate the section on Se.
The sections on P and S are shorten as suggested by Rev.1.
Interference cases are revisited for CNPS only.
Eq.1 is reformulated.
Details on the SV-ICPMS instrumentation are also given.
Recommendations are given…

Reviewer 2

Thank you for the additional references
Most of the references deal with cells and not viruses, except the last one which is added to the ref.s list.
Eq 1 is upgraded and symbols clarified…
Phosphorus is corrected

Highlights

- Single particle (SP) ICP-MS may be applied to analyse interference-free single viruses (SV).
- SV ICP-MS analysis is performed with master ions (main elements) and key ions (P, S, Se, ..).
- 2 to 500 single viruses can be counted and analysed in 20 s by single viruses ICP-MS.
- C and N/C, P/C and S/C molar ratios are analysed for SARS-COV9 and T5 Sipho viruses
- A data bank of virus C amount and N/C, P/C, S/C … molar ratios will be needed.

Click here to access/download;Graphical Abstract (for review);SV ICPMS Graph Abstr 20 01 21(1).pdf

Single Virus Inductively Coupled Plasma Mass Spectroscopy

Injection strategy: Virus suspension in ultrapure water flow

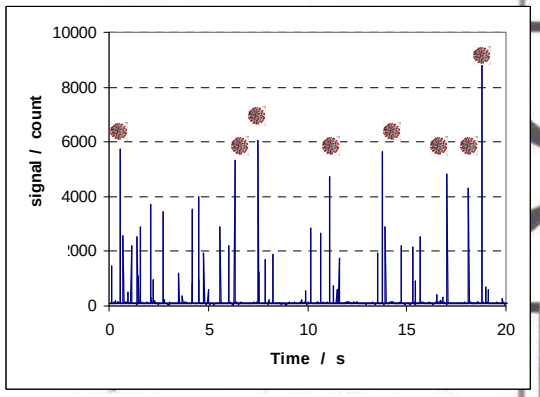

Reading in 20 sec

$I_{Master\text{-}ion}$ & $I_{key\text{-}ion}$

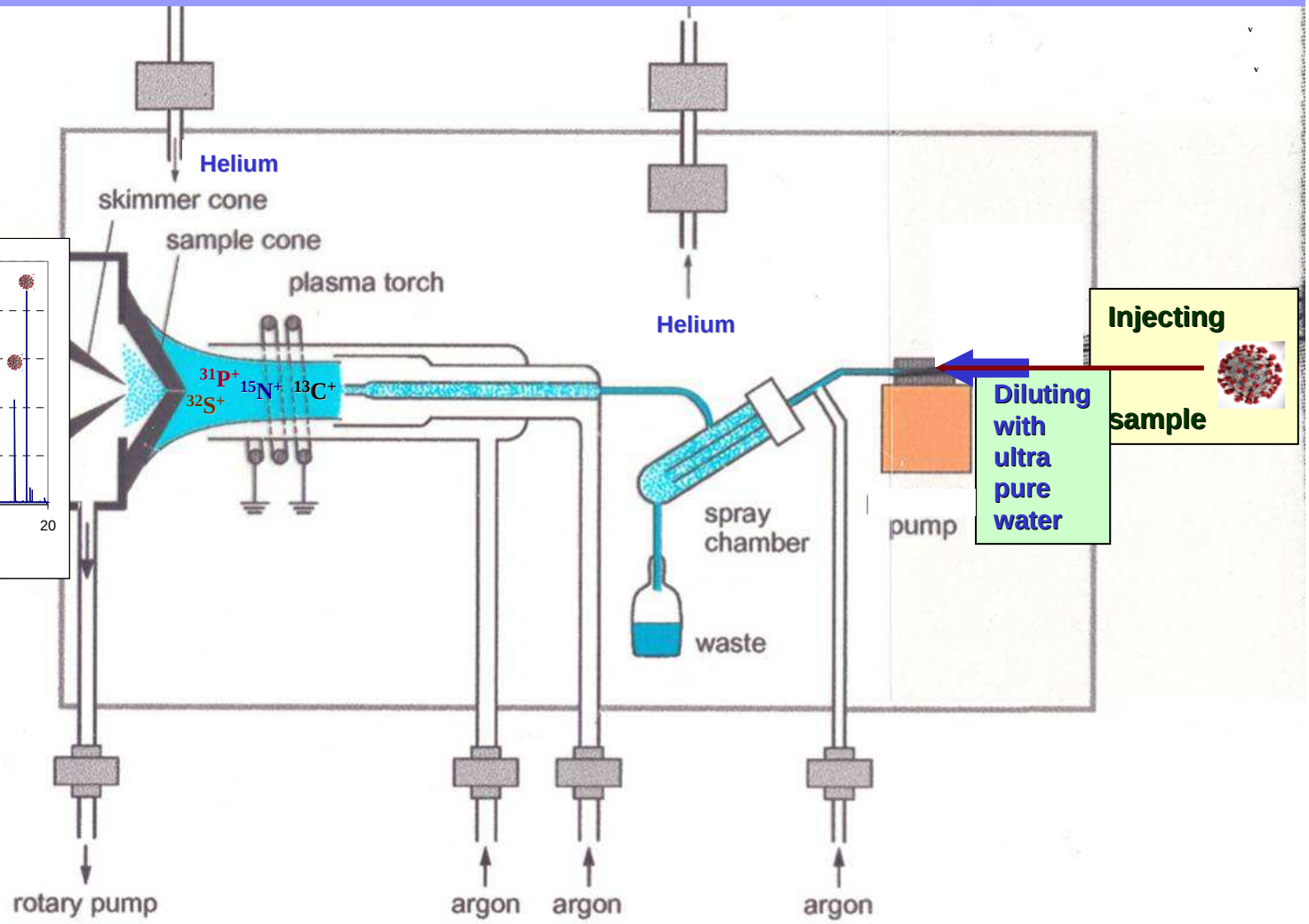

Viruses analysis is performed in a single virus sector field ICP-MS unit for $^{12}C^+$ or $^{13}C^+$ and $^{14}N^+$ or $^{15}N^+$, and for $^{31}P^+$ and $^{32}S^+$, using a multi-channel unit. The detection rate may be of 2-500 viruses in 20 s. High resolution MS avoids isobaric interferences.

NEW Revised Manuscript [Unmarked Text]

Single virus inductively coupled plasma mass spectroscopy analysis: a comprehensive study.

Claude Degueldre
Engineering Department, Lancaster University, Lancaster LA1 4YW, UK
c.degueldre@lancaster.ac.uk

Abstract

The characterisation of individual nanoparticles by single particle ICP-MS (SP-ICP-MS) has paved the way for the analysis of smallest biological systems. This study suggests to adapting this method for single viruses (SV) identification and counting. With high resolution multi-channel sector field (MC SF) ICP-MS records in SV detection mode, the counting of master and key ions can allow analysis and identification of single viruses. The counting of 2-500 virial units can be performed in 20 s. Analyses are proposed to be carried out in Ar torch for master ions: $^{12}C^+$, $^{13}C^+$, $^{14}N^+$, $^{15}N^+$, and key ions $^{31}P^+$, $^{32}S^+$, $^{33}S^+$ and $^{34}S^+$. All interferences are discussed in detail. The use of high resolution SF ICP-MS is recommended while options with anaerobic/aerobic atmospheres are explored to upgrade the analysis when using quadrupole ICP-MS. Application for two virus types (SARS-COV2 and bacteriophage T5) is investigated using time scan and fixed mass analysis for the selected virus ions allowing characterisation of the species using the N/C, P/C and S/C molar ratio's and quantification of their number concentration.

Keywords: Virus identification; virus counting; SP ICP-MS; individual virus analysis; single virus ICP-MS.

1. Introduction

Single particle inductively coupled plasma mass spectroscopy (SP ICP-MS) was first tested at Institute Forel, University of Geneva in 2001 and presented in 2002 at the EMRS Spring Meeting in a proceedings paper published by Degueldre and Favarger [1]. This method was later tested on gold nano- particles that are used as substrate in nano- pharmacy, and published subsequently i.e. Degueldre *et al* [2]. SP ICP-MS was also tested on dioxides e.g. Degueldre *et al* [3,4,5]. The characterisation of individual metallic nanoparticles by ICP-MS analysis has been carried out by laser ablation as reviewed by Koch and Günther [6] or by so-called single particle ICP-MS which has paved the way for the analysis of small biological systems like individual microscopic cells e.g. Zheng *et al* [7] and Corte-Rodríguez *et al* [8]. Today the challenge of very sensitive ICP-MS methods is to solve specific medical issues such as contaminations pathways or viruses spreading and the role of forgotten elements e.g. Te as pointed out by Amais *et al* [9]. This conceptual study suggests the use this method for single viruses (SV) ICP-MS identification and counting. Its potential is tested for two virus kinds: one of RNA and one of DNA type.

2. Methodology

To perform SV ICP-MS high dilution of the viral sample suspension is required to inject one virus at a time in the plasma torch, producing one flash of ions per slot time of the Mass Spectrometer. After atomisation/ionisation in the plasma torch the flash of ion (cloud) passes through the conus pin hole and is analysed in the mass spectrometer. The number of flash is proportional to the concentration of viruses in the sample, and the intensity of the ionic flash is proportional to the fraction of the element (isotope ion) present in the viral object. For practical reason one considers the argon (Ar) plasma torch.
In nanomedicine virus analysis is a key issue, however current molecular analysis is usually time consuming. In this study for virus identification one is interested to discriminate the fraction of master ions (atoms from the matrix of the virus) and the fraction of key element (ion from a coating e.g. drug, or from a selected element e.g. specific for given amino acid or for the viral RNA or DNA). In the case of a given virus, for example, SV ICP-MS shall require the selection of one (or two) master ion(s) and of 2 key ions to identify them and quantify their fraction in the virus 'body'.
In ICP-MS analyses the introduced sample is largely ionized in the plasma followed by a separation of the ions by their mass-to-charge ratio. A resulting ion beam is then quantified via calibration of the associated signal intensities. Usually the argon plasma is operated under atmospheric conditions and the analytes are transported there either in acidified (or basic) aqueous solution or in organic solvents, the most abundant elements in the plasma next to Ar are H, O, N, and C. To reduce contamination (C,N,O) the torch is placed in argon atmosphere. Table 1 provides standards experimental conditions to perform SP ICPMS analysis.

Table 1 Typical Instrument and operating conditions for ICP-MS

Radio frequency applied power (kW)	1.4
Plasma gas flow rate (L min^{-1})	18.0
Nebulizer gas flow rate q_{neb} / (L min^{-1})	1.0
Auxiliary gas flow rate / (L min^{-1})	1.8
Sheath gas flow rate / (L min^{-1})	0.13
Sampling depth / (mm)	5.5
Ultra pure water flow rate (mL min^{-1})	200
Sample injection flow rate (mL min^{-1})	0.20
Replicates *per* sample	5
Spray chamber temperature / (°C)	2
Mass-to-charge ratio (*m/z*) master ions	12, 13, 14, 15,

Mass-to-charge ratio (*m/z*) key ions	31, 32, 34,
Scan mode	Time
Acquisition mode	Multi-channel, fixed masses, time-scan

Since the quadrupoles can be tuned to select for different masses, they are ideally suited for the interferences. The first mass filter is then set to the analyte plus its interference, e.g. m/z 32 for sulphur, after the reaction cell e.g. A+1 with H of H_2 and A+16 with O of O_2.

A little intensity is lost through the process, but the gain is worth the loss: interference being drastically lowered, the collision/reaction cell's performance is at its best level. The advantages and disadvantages of ICP-MS is its very large range of analysis, however SV ICP-MS remains a non-species selective analysis.

On the other hand, in a known matrix with a known analyte, a very accurate quantitation can be performed by the mean of a conversion factor for calculation of the species of interest. If a soluble or gaseous interferes in the scan signal (background), it can be reduced by dilution in the stream of pure water used in SV mode. The advantage of this method is the principle of analysis itself that gets rid of organic compounds that could interfere in other types of measurements by a digestion step (solid samples) and/or directly by the subsequent plasma ionization.

Multi-Channel (MC) ICP-MS allows, compared to simple quadrupole ICPMS, a finer analysis due to the addition of a supplementary quadrupole to the system before the collision / reaction cell. This addition acts as a supplementary mass filtering unit thus removing more of the interferences. Use of a sector field (SF) improves also widely the technique (better resolution, multi -channel analysis).

Since today's sector field MC ICP-MS (see Fig. 1) can detect some atoms (say 5-20 ions per ion flash and per channel) the potential of this technique is impressive. However, a full analysis of the potential interfering ions is mandatory.

Fig. 1: Single Virus Multi-Channel Inductively Coupled Plasma Mass Spectrometry SV MC ICP MS adapted for master ions and key ions analysis. Note the dilution factor used when injecting the sample (syringe) in the stream of pure water, see Degueldre and Favarger (2003).

2.1 Virus master ion analysis

The virus major ions are those ions from the main elements of the virus in the membrane, S-protein, lipid layers, capsid as well as in the nucleic (RNA or DNA) core. These elements are H, C, N and O. For the mass spectrometer of the ICP-MS, ion isotopes detected shall be $^{12}C^+$, $^{13}C^+$, $^{14}N^+$, $^{15}N^+$. They are reported in Table 2 with their potential interferences in the Ar plasma. H and O isotopes are not considered because they are due to water itself from the solution and from the hydration of the viral object. Note that the dissolved (and the low molecular suspension) molecules appear in the MS reading as a continuum and that the SV and SP signals are ion peaks. Interferences on $^{A}X^+$ are easy to sort out; they are $[^{A/2}X'_2]^+$, $[^1H^{A-1}X']^+$, $[^1H_2{}^{A-2}X']^+$, $^{nA}X'^{n+}$, where X' is the interfering element isotope of mass derived from ^{A}. Potential interferences are reported in Table 2. Their masses give their potential of interference on the mass scale and their abundances guide the overlapping effect they may have in the intensity scale.

2.1.1 Measuring carbon

For $^{12}C^+$ the interferences (given in Table 2) may be: $[^6Li_2]^+$, $[^1H^{11}B]^+$, $^{24}Mg^{2+}$and $^{48}Ti^{4+}$, however these elements may be absents or very diluted in the suspension. Only $^{36}Ar^{3+}$ could interfere, however its abundancy is 0.337% in Ar reducing its impact and its triple ionisation may be avoided at lower plasma temperature which are usually several orders of magnitude greater than the temperature of the neutral species, see Shun'ko *et al* [10]. With a mass difference of 0.007 $^{24}Mg^{2+}$ may interfere with $^{12}C^+$, however, dilution is possible when Mg is soluble. Otherwise the reaction cell described below for $^{13}C^+$ is applicable.

For $^{13}C^+$ the interferences (given in Table 2) may be: $[^1H^{12}C]^+$, $[^2H^{11}B]^+$, $^{26}Mg^{2+}$ and $^{39}K^{3+}$. The solution must be exempted of B, Mg and K. If one of these ions interferes as soluble it may be further diluted to reduce the background without affecting the height of the single particle peaks. Decreasing slightly the flow rate of the aerosol gas from that which yields maximum signal eliminates this $^{12}C^1H^+$ interference as reported by Luong and Houk [11]. Additional information is given in Table 2. Clearly with a mass difference of 0.005 $[^1H^{12}C]^+$ may interfere with $^{13}C^+$. For oxide-forming analytes, this can be achieved elegantly in a reaction cell by the means of oxygen. This interference may be avoided by forming $^{13}C^{16}O^+$ using the reaction:

$^{13}C^+ + {}^{16}O_2 \rightarrow {}^{13}C^{16}O^+ + {}^{16}O$

Actually, the formation of $^{28}Si^+$ from the quartz vessel may interfere on $^{12}C^{16}O^+$ as well as the formation of $^{30}Si^+$ (low abundance) could interfere on $[^1H^{13}C^{16}O]^+$ (low probability of formation). Consequently the use of SF ICP-MS may be suggested.

2.1.2 Measuring nitrogen

For $^{14}N^+$ the interferences may be: $[^7Li_2]^+$, $[^2H^{12}C]^+$ and $^{28}Si^{2+}$. Basically lithium should be in the soluble phase and dilution shall reduce the effect, $^1H_2{}^{12}C$ may be originating from the soluble and particulate (virus) phase and Si could also be part of the soluble phase (soluble SiO_2 or silicates) or from the particle phase e.g. quartz fragments or from the torch. Ultra-traces of N_2 in the carrier gas is also an issue (see discussion). Details are given in Table 2.

For $^{15}N^+$ the interferences may be: $[^1H^{14}N]^+$, $^{30}Si^{2+}$ and $^{60}Ni^{4+}$. Basically HN may be originating from the soluble and particulate (virus) phase and Si could also be part of the soluble phase (soluble SiO_2 or silicates) or from the particle phase e.g. quartz fragments from the nebuliser/torch vessel. Details are given in Table 2. Here the mass differences (N^+ and interference) are larger than 0.008 and the use of high resolution MS is suggested.

Table 2: Master ion isotopes and their interferences considered for the SV ICP-MS analysis. Molecular mass $\mathcal{M}({}^{A}[X]^{+})$ of ${}^{A}[X]^{+}$ and its abundance: Abd.

Isotope ^{A}X	$\mathcal{M}({}^{A}[X]^{+})$	Abd (%)	Interference	$\mathcal{M}({}^{A}[YZ]^{+})$, $\mathcal{M}({}^{nA}[Y]^{n+})$	Abd (%)
^{12}C	11.99945	98.900	$[^{1}H^{11}B]^{+}$,	12.01659	80.09
			$^{24}Mg^{2+}$,	11.99252	62.39
			$^{36}Ar^{3+}$,	11.98863	00.337
			$^{48}Ti^{4+}$,	11.98644	73.8
^{13}C	13.00280	01.100	$[^{1}H^{12}C]^{+}$,	13.00728	98.885
			$^{26}Mg^{2+}$,	12.99075	11.01
			$^{39}K^{3+}$,	12.98735	93.258
^{14}N	14.00252	99.634	$[^{1}H^{13}C]^{+}$,	14.01008	01.998
			$^{28}Si^{2+}$,	13.98702	92.23
^{15}N	14.99956	00.366	$[^{1}H^{14}N]^{+}$,	15,01063	99.619
			$^{30}Si^{2+}$,	14.98634	03.10
			$^{60}Ni^{4+}$,	59.930785	26.223

All these interferences may also be avoided using high resolution MS.

2.2 Virus key ion analysis

The virus key ions are those from these elements that characterise its properties and functionalities. Phosphorus is an integral part of the nucleotides and thus of all fragments of DNA and RNA, so it can be used to quantify such macromolecules. Sulphur is present in large molecules, either as active groups, e.g. in thiols, or within the normal structure of specific amino acids. In SV analysis it is consequently essential to quantify the elemental fractions of these elements.

The key ion isotopes are subject like major element to interferences. The more relevant isobaric interferences are given in Table 3. Interferences on $^{A}X^{+}$ are easy to evaluate; these are $[^{A/2}X'_{2}]^{+}$, $[^{1}H^{A-1}X']^{+}$, $[^{1}H_{2}{}^{A-2}X']^{+}$, $^{nA}X'^{n+}$, but also $[^{16}O^{A-16}X']^{+}$ and $[^{16}O_{2}{}^{A-32}X']^{+}$.

The low mass-range of the ICP-MS is very "crowded" by $[NO]^{+}$, $[O_2]^{+}$, $[CO]^{+}$, varying in their mass by the combination and abundance of their respective fractions. For example, $[^{16}O_2]^{+}$ with the mass 32 is very common, and while $[^{15}O_2]^{+}$ with 30 is much less abundant, $[^{14}N^{16}O]^{+}$ also contributes at this mass. In case the mass of interest is affected by such polyatomic interferences, an effective way to solve the interference is needed. The solution is to work in a He atmosphere surrounding the Ar torch system avoiding the N_2, O_2 and CO_2 contamination of the system. Some of these cluster ions may interfere with the measured key ions $^{31}P^{+}$, $^{32}S^{+}$ and $^{33}S^{+}$.

2.2.1 Measuring phosphorus

Phosphorus is a mono-isotopic element of mass 30.97 amu. For a mass-based analytical technique like ICP-MS, this means that only the one isotope (^{31}P) can be selected to quantify phosphorus. For $^{31}P^{+}$ the interferences are given in Table 3.

The phosphorus analysis by ICP-MS is somewhat limited by a weak detection limit, as reviewed by Martínez-Sierra, *et al* [12]. Since their detection limit is weak in current argon plasma troch a variant is mandatory. Measuring option is to use the ICP-MS - O_2 reaction cell to analyse phosphorus.

For phosphorus, which receives strong interference from multiple ions (like $[^{15}N^{16}O]^+$, $[^1H^{14}N^{16}O]^+$, $[^{13}C^{18}O]^+$, ...) or $^{62}Ni^{2+}$ see Table 3, a solution may be a mass shift from 31 to 47 amu with:

$$^{31}P^+ + {}^{16}O_2 \rightarrow [^{31}P^{16}O]^+ + {}^{16}O$$

For the interfering species, mass remains 31 amu:

$$[^{15}N^{16}O]^+ + O_2 \rightarrow \text{no reaction}$$

However, it must be kept in mind that although the analyte can then be analyzed at a mass different to its interfering species, the mass it is shifted to could be already be "occupied" by other analytes also present in the sample, e.g. ^{47}Ti in the case of $[^{31}P^{16}O]^+$. In such cases, with a normal single quadrupole ICP-MS system, one would end up with the same problem, just at another mass.
Interferences may also be avoided using high resolution MS.

2.2.2 Measuring sulphur

The phosphorus and sulfur analysis by ICP-MS is somewhat limited by a weak detection limit, as reviewed by Martínez-Sierra, *et al* [12]. A method for the analysis on-line of species-specific sulfur isotopes by means of multi-collector ICP-mass spectrometry has been proposed by Faßbender, *et al* [13]. Since their detection limit is weak in current argon plasma troch a variant is mandatory. Measuring option is to use the ICP-MS – O_2 reaction cell to analyse sulphur.

For sulphur, three naturally stable isotopes (^{32}S, ^{33}S, ^{34}S) are found with an abundance of approximately 95% for ^{32}S. For the determination of trace concentrations, the only reasonable isotope is offered by ^{32}S. Their high resolution mass spectra are presented Fig 2. For sulfur, which receives strong interference from the ion $[^{16}O_2]^+$ as well as $[^1H^{31}P]^+$, $^{64}Zn^{2+}$, $^{96}Mo^{3+}$, and $^{64}Ni^{2+}$ (the later if Zn, Mo or Ni (cone) are present) a mass shift from 32 to 48 amu is suggested using a reaction cell:

$$^{32}S^+ + {}^{16}O_2 \rightarrow {}^{32}S^{16}O^+ + {}^{16}O$$

While the interfering ion mass remains 32 amu for $^{16}O_2$.
However, it must be kept in mind that although the analyte can then be analyzed at a mass different to its interfering species, the mass it is shifted to could be already be "occupied" by other analytes also present in the sample, e.g. $^{48}Ti^+$ in the case of $[^{32}S^{16}O]^+$. In such cases, with a normal single quadrupole ICP-MS system, one would end up with the same problem, just at another mass. Interferences may also be avoided using high resolution MS.

Table 3: Key ion isotopes considered for the SV ICP-MS analysis. Molecular mass $\mathcal{M}(^{A}[X]^{+})$ of $^{A}[X]^{+}$ and its abundance Abd.

Isotope ^{A}X	$\mathcal{M}(^{A}[X]^{+})$	Abd (%)	Interference $\mathcal{M}(^{A}[YZ]^{+})$, $\mathcal{M}(^{2A}[Y]^{2+})$	Abd (%)
^{31}P	30.97321	100.000	$[^{15}N^{16}O]^{+}$ 30.9945	00.365
			$[^{1}H^{14}N^{16}O]^{+}$ 31.0091	99.382
			$[^{13}C^{18}O]^{+}$ 31.0026	00.022
			$^{62}Ni^{2+}$ 30.9642	03.634
^{32}S	31.97152	95.02	$[^{1}H^{31}P]^{+}$, 31.98104	99.985
			$^{64}Zn^{2+}$, 31.96402	48.60
			$[^{16}O_2]^{+}$ 31.98927	99.525
			$^{64}Ni^{2+}$ 31.9640	00.926
^{33}S	32.97091	0.75	$[^{1}H^{32}S]^{+}$ 32.97935	95.006
^{34}S	33.96732	4.21	$[^{16}O^{18}O]^{+}$ 33.99352	00.199

Fig. 2: Discriminating $^{A}S^{+}$ and their interferences by HR MC ICPMS Ref. Martínez-Sierra, *et al* [30].

Un-labelled virus identification may consequently be done by measuring master ions and the key ions. The first give a weight of carbon, nitrogen and oxygen and could be used to derive a total mass (in Da) of the virus, on the basis of calibration. The oxygen data may be affected by the virus hydration grade. The key ion data allow by deduction identification of the virus based on its functionalities derived from specific amino acids present in the virus. In all case the concentration of the virus (in number per mL) can be deduced.

3. Application and discussion

3.1 Application of the single particle methodology

Single particle inductively coupled plasma mass spectrometry (SP-ICP-MS) offers unique features for the detection of particles, as well as for their quantification and size characterization. The detection capabilities of SP-ICP-MS are therefore not only limited to the concentration domains (of particles and dissolved related species), but also to the mass of element per particle and particle size domains as reported by Degueldre & Faverger (2003) and confirmed by Laborda *et al* [14]. Discrimination and detection of particle events, based on the use of robust limits of decision and the estimation of the limits of detection in the different domains, require standardized metrological approaches that have not been clearly established yet. As a consequence, harmonized approaches and expressions to allow reliable comparisons between methods and instruments, as well as to process SP-ICP-MS data, are required.

ICP-MS is a powerful method, unfortunately, the linear dynamic range of single particle analysis may be hindered by “unruly” transient signals and momentary pulse pile-ups at the electron multiplier detector see Rush *et al* [15]. This study investigated a way to extend the dynamic range of ICP-MS nano-particle quantification *via* addition of a collision gas in the

collision cell of the ICP-MS. The collision gas temporally broadens the nano-particle signal resulting in decreased pulse pile-up and increased integrated intensity, up to a point where scattering losses begin to dominate. The addition of a collision gas used together with the dual mode detector shows a promising path forward towards mitigating unruly transient signals, improving the dynamic range of nano-particle quantification.

Non-spectral interferences in single-particle ICP-MS analysis is another underestimated phenomenon according to Loula *et al* [16]. Spectral and non-spectral interferences in inductively-coupled plasma mass-spectrometry were investigated by Dams *et al* [17]. Non-spectroscopic effects of organic compounds were also investigated by Kralj and Veber [18].

Single-particle ICP-MS method was validated by Witzler *et al* [19] to measure nano-particles in human whole blood for nano-toxicology. A highly efficient introduction system for single cell- ICP-MS and its application to detection of copper in single human red blood cells has been reported by Cao *et al* [20].

The number of X ions N_X (-) for a single virus $C_\chi H_\eta O_\omega N_\nu P_\pi S_\sigma$ (with ξ: χ, η, ω, ν, π, and σ the stoichiometric coefficient of X: C, H, O, N, P or S) of size d_{vir} (cm) is given by:

$$\xi = N_X = \frac{\xi \pi d_{vir}^3 \rho N_{Av}}{6 M(vir)} \qquad (1)$$

where ρ (g cm^{-3}) is the virus density, N_{Av} the Avogadro constant (mol^{-1}), the virus molecular weight $\mathcal{M}_{(C_\chi H_\eta O_\omega N_\nu P_\pi S_\sigma)}$ (simplified as M(vir)).

The number of atoms N_X is also deduced from the signal $s_A(t)$ during its appearance (between t_1 and $t_1+\Delta t$, with Δt the full peak time) by the expression:

$$N_X = \frac{1}{\eta_A \eta_C} \int_{t_i}^{t_i+\Delta t} s_A(t)\, dt \qquad (2)$$

With η_A for ^{A}M the isotopic abundance and η_c the counting efficiency.
The virus number concentration N_{vir} (mL^{-1}) in the original suspension is diluted by a factor q_{vir}/q_{sol}. The fraction η_{neb} is found in argon, which mass flow is q_{Ar}. The dilution is only valid for the dissolved species. However, the virus as single entity remains entire and is not diluted. Its appearance frequency $f(s_A)$ (s^{-1}) of virus ion flashes in the torch is given by:

$$f(s_A) = N_{vir}\ q_{vir}\ \eta_{neb} \qquad (3)$$

These equations allow evaluation of the size distribution for a given element/isotope in the virus phase to be evaluated.

Now the SV-ICP-MS method has a very powerful potential with the possibility to analyze 2 to 500 viral objects in 20 s which can be explored for 2 kinds of viruses as examples.

3.2 Single virus data analysis

A virus is a composite object that may be characterized by its chemical composition, which chemical formula reads:

$$C_\chi H_\eta O_\omega N_\nu P_\pi S_\sigma,$$

with χ, η, ω, ν, π, and σ the stoichiometric coefficient of C, H, O, N, P and S respectively. In SV analysis it is essential to quantify the elemental fractions of these elements. They are

constituents of specific amino acids, some of which are reported in Table 4. These are the constituents of proteins.

The molecular weight of the virus M(vir) is calculated as:

$$M(vir) = \chi\, \mathcal{M}(C) + \eta\, \mathcal{M}(H) + \omega\, \mathcal{M}(O) + \nu\, \mathcal{M}(N) + \pi\, \mathcal{M}(P) + \sigma \mathcal{M}(S) \quad (4)$$

It may be evaluated from the mass of fragments and their composition of these virus parts. Their chemical composition is estimated within a variation that can be of the order of easily 10%. Table 4 gives some key components of living mater.

The SV ICP MS time scan can be recorded and analysed for the elements: C, H, O, N, P and S as follows.

Table 4: Amino acids (AA) with P and S as key ions and nucleo-bases.

	Amino acid	**Ions**	**Formula**	$\mathcal{M}$**(AA)**	**Key/master ion ratio**
SEP (S)	**Phosphoserine**	P^+	$C_3H_8NO_6P$	185.073	1/18
TPO (T)	**Phosphothreonine**	P^+	$C_4H_{10}NO_6P$	199.10	1/21
PTR (Y)	**O-phosphotyrosine**	P^+	$C_9H_{12}NO_6P$	261.17	1/27
CSO (C)	**S-hydroxycysteine**	S^+	$C_3H_7NO_3S$	**137.16**	1/14
HIP (H)	**Cysteine**	S^+	$C_3H_7NO_2S$	121.16	1/13
TAU (J)	**Taurine**	S^+	$C_2H_7NO_3S$	125.15	1/13
	Nucleo-bases				
A	**Adenine**	C^+, N^+, O^+	$C_5H_5N_5$	135.1267	-
T	**Thymine**	C^+, N^+, O^+	$C_5H_6N_2O_2$	126.04	-
C	**Cytosine**	C^+, N^+, O^+	$C_4H_5N_3O$	111.102	-
G	**Guanine**	C^+, N^+, O^+	$C_5H_5N_5O$	151.1261	-
U	**Uracil**	C^+, N^+, O^+	$C_4H_4N_2O_2$	112.0867	-

The carbon peaks allow a pre-evaluation of the virus molecular weight on the basis of the signal integration, the calculation of the mass of carbon in the virus and evaluation the virus mass from a standard virus molecular formula ($C_\chi H_\eta O_\omega N_\nu P_\pi S_\sigma$). A pre-identification may be derived following the classification proposed by Matthews [21]. For 59 different viruses, when the amount of nucleic acid in the particle is related either to the dry weight of the particle or to the particle volume, two classes of virus groups emerge - those with enveloped or those with geometrical particles.

Now let us examine the chemical association of the major and key ions in the virus phases.

Viral oxygen is linked to acidic, alcoholic, ketonic groups of bio compound but first to virus hydration (water), to be linked with the density i.e. real virus density or weight and virus anhydrous density or weight.

Viral nitrogen is associated to basic groups of bio compounds, i.e. ATCG (DNA) or ATCU (RNA) and specific amino acids.

Viral phosphorus is due to phosphate acid groups of bio compounds, it should be possible to distinguish DNA from RNA viruses and also phosphor- serine, threonine and tyrosine rich proteins.

Viral sulphur is found for thiol, thio-ketone groups of bio compounds as well as cysteine, methionine and taurine rich proteins.

Knowing the fractions the viral formula $C_\chi H_\eta O_\omega N_\nu P_\pi S_\sigma$ may be deduced from the SV ICP-MS peaks and the virus molecular weight.

Viruses belonging to the family *Coronaviridae* consists of species that are first recognised for their specific morphology (TEM), see for example Fig. 3. The characterization of spike proteins from viruses is of course important for antiviral drug development e.g. Shanker, *et al* [22]. For SARS-CoV-2 the viruse's functions are dictated by its RNA. *Coronaviridae* protein compositions have been analysed since several decades e.g. Hierholzer, *et al* [23] for the coronavirus OC 43. The buoyant density in potassium tartrate of the virus was 1.15 g cm^{-3} and of the intact OC 43 virion was 1.18 g cm^{-3}. By analytical ultracentrifugation the corrected sedimentation coefficient of the OC 43 virion was determined and the apparent molecular weight (M(vir)) was calculated to be (112 ± 5) x 10^6 Da. The human respiratory coronavirus OC43 was isotopically labelled with amino acids, glucosamine, and orthophosphate to analyze virion structural proteins as reported by Hogue and Brian [24]. Major protein species were resolved by electrophoresis and many of their properties were deduced from digestion studies using proteolytic enzymes.

The first virus investigated in this work, the SARS-COV 2 virus was chemically described recently by Popovic & Minceva [25]. RNA and protein data utilized in this work are given in Table 5. Note that the number of protein copies per virion varies, even within a single species, as reported by Neuman *et al* (2011)[[26]. For example, the number of spike protein trimers can vary between 50 and 100 per virion. The average number is 74 trimers, giving 74 × 3 = 222 spike proteins in total, see Neuman *et al* (2006) [27]. Total number of atoms constituting the viruses is gained by the atom counting method. For each virus, the number of atoms is given for the entire virion (nucleocapsid + envelope) and the nucleocapsid. The last line presents the molar mass of entire virions, in Daltons.

Fig. 3: Negative stain electron microscopy SARS-COV 2 showing spikes, membrane, capsid and RNA genome. Adapted from Humphrey [28]. Biochemical composition, see Table 5.

The empirical formula of RNA was taken to be the average RNA of all RNA viruses considered in the atom counting method $CH_{1.2316}O_{0.7610}N_{0.3967}P_{0.1050}$.
The protein composition was taken as the average viral protein composition of all viruses considered in the atom counting method $CH_{1.5692}O_{0.3085}N_{0.2708}S_{0.0061}$, lipid composition was represented by that of human lipids $CH_{1.9216}O_{0.1176}$,see Wang *et al* [29] and non-nucleic acid carbohydrate composition may be represented by the empirical formula of carbohydrates CH_2O.

Table 5: Components, chemical formula and masses of a SARS-COV-2 virus. Genome: Sense: → , Bases: A T C U , POD: phosphate desoxyribose.

Component	Formula	Mass (Da)	Subunit	Mass tot (Da)
Nucleoprotein Total	$C_{1971}H_{3137}N_{607}O_{628}S_7$ $C_{4667328}H_{7428416}N_{1437376}O_{1487104}S_{16576}$	45,625	2368	108,040,000
Membrane protein Total	$C_{1165}H_{1823}N_{303}O_{301}S_8$ $C_{1379360}H_{2158432}N_{358752}O_{712768}S_{9472}$	25,146	1184	29,772,864
Spike protein Total	$C_{6336}H_{9770}N_{1656}O_{1894}S_{54}$ $C_{1406592}H_{2168940}N_{367632}O_{420468}S_{11988}$	141,175	222	31,340,850
Total Protein	$C_{7453280}H_{11755788}N_{2163760}O_{2620340}S_{38040}$	-	-	169,153,714
Genome	$\rightarrow A_a T_t C_c U_u$			
Genome total	$C_{2646720}H_{4804202}N_{161240}O_{260660}P_{65230}Na_{65230}$	46,514,892	1	*52,346,286*
Virus total	$C_{10100000}H_{16560000}N_{2325000}O_{2881000}P_{65230}S_{38040}Na_{65230}$		1 filled capsid	221,500,000

The second examined case is the *Siphoviridae* bacteriophage T5 virus which morphological characteristics are depicted Fig. 4 and chemical composition reported in Table 5. The huge 105 MDa DNA-filled viral particle mass was accurately measured using a nano-mechanical mass spectrometer as reported by Domingez-Medina [30]. DNA was taken to be the average DNA of all DNA viruses considered in the atom counting method $CH_{1.2555}O_{0.5840}N_{0.3796}P_{0.1022}$.

Fig. 4: Morphological characteristics of the *Siphoviridae* bacteriophage T5 virus, adapted from Domingez-Medina (2018) [30]. Biochemical composition, see Table 6.

Table 6: Components, chemical formula and masses of a *siphoviridae* bacteriophage T5. Genome: Sense: →, antisense: ←, Bases: A T C G , POD: Na phosphate desoxyribose.

Component	Formula	Mass (Da)	Subunit	Mass tot (Da)
Head protein pb8	$C_{1466}H_{2349}N_{391}O_{445}S_5$	32,892	775	25,491,633
Total	$C_{1136150}H_{1820475}N_{303025}O_{344875}S_{3875}$			
Portal protein pb7	$C_{1948}H_{3099}N_{523}O_{601}S_{13}$	43,879	12	526,548
Total	$C_{23376}H_{37188}N_{6276}O_{7212}S_{156}$			
Empty capsid				26,018,181
Head completion protein p144	$C_{853}H_{1352}N_{224}O_{263}S_8$	19,210	12	230,521
Total	$C_{10236}H_{16224}N_{2688}O_{3156}S_{96}$			
Total proteins	$C_{1169762}H_{1873887}N_{311989}O_{355243}S_{4127}$			26,248,702
Genome bases	$\rightarrow A_{36051}T_{37888}C_{23473}G_{24388}$ $C_{20}H_{35}N_7O_8Na_2P_2$	650	121,750	79,137,500
	$\leftarrow A_{37888}T_{36051}C_{24388}G_{23473}$	*620*	*121,800*	*75,516,000*
Genome Elements	→ $C_{585527}H_{609790}N_{438390}O_{123637}$			
	← $C_{584612}H_{609000}N_{452071}O_{119963}$			
	POD: $C_{1218000}H_{569000}O_{121800}P_{243600}Na_{243600}$			
Genome total	$C_{2388139}H_{29971390}N_{900461}O_{1905200}P_{243600}Na_{243600}$		1	
Virus total	$C_{3557901}H_{4871277}N_{1212450}O_{2260443}P_{243600}S_{4127}Na_{243600}$		1	105,386,202

The researchers measured hundreds of DNA-filled viruses and found that the normalised distribution of measured masses centred on 108.4 MDa. This value is slightly higher than the calculated molecular mass of 105.4 MDa, perhaps because of salt introduced during ionisation, or the degree of hydration.

Application of SV ICP-MS

The full calculation of a SV ICP MS may be estimated as follow:

1. establish the molecular formula $C_\chi H_\eta O_\omega N_\nu P_\pi S_\sigma$ of the virus
2. with Eq 1 and 2 derive the peak characteristics,
3. with Eq 3 derives the number of peak per time unit from the virus number concentration in the original sample.

Figure 5 shows the scan that can be recorded for the 2 virus types studied in this work.
The peak intensity recorded for ^{13}C, ^{15}N, ^{31}P, ^{32}S can be used to identify the virus, and the frequency in the scan is directly proportional to the virus concentration.

For the COV-2 virus, the molar ratio's are:

N/C = 0.230; P/C = 0.0065 and S/C = 0.00377.

For this RNA virus, the single rather short genome chain contributes to a small P/C ratio and a slightly reduced N/C ratio compared to the *siphoviridae* case treated below. The COV-2 is however known to be rather sulphur rich and the S/C ratio is larger here than for the bacteriophage T5 (DNA virus).

For the *siphoviridae* (DNA virus) the ratios are:

N/C = 0.313; P/C = 0.0684 and S/C = 0.0012.

Mass fractions are often used in human body composition research, for example the composition of an average adult is 21.0% C, 10.2% H, 63.7% O, 2.7% N, 0.7% P, 0.2% S and 1.6% other elements, see Wang *et al* (1993) [29].
The human body molecular average ratio's are:

N/C = 0.11; P/C = 0.013 and S/C = 0.0036.

Fig. 5: Simulated SV ICP MS scan for analysis of Viruses.
a. 24 single SARS COV-2 viruses +2 counted as double
b. 16 single *siphoviridae* bacteriophage T5 viruses +1 counted as double.
Conditions: recording time 2 s, Δt: 10 ms, η_C : $2x10^{-2}$, η_A: $^{13}C^+$: 1.10%, $^{15}N^+$: 0.366%, $^{31}P^+$: 100%, $^{32}S^+$: 95%, other conditions see Table 1. Readings: **a.** at 0.26 s and 1.95 s: aggregates of 2 viruses, 1.38 bio-fragment e.g. cellulose nano particle, **b**. at 0.42 s: aggregate of 2 viruses, for **a.** & **b.** the $^{13}C^+$ background is due to residual DOC and traces of CO_2, the $^{15}N^+$ background is due to residual dissolved N_2 in solution and traces of N in DOC.

Recommendations
The single virus analysis challenge is to discriminate the C and N ICP-MS peaks from the virus from the C and N signal backgrounds. Clearly reduction of both background signals is possible working in a helium glove box (also required to avoid viral contamination) and using argon for the plasma torch with at least a seven 9 quality argon at least during sample injection. The argument C and N analysis by ICPMS is not possible is wrong this is due to the air contamination because ICP-MS analysis is traditionally carried out in atmospheric conditions. Actually C and N analyses are possible e.g. Riisom, *et al* [31]. Reduction of both C (CO_2 and TOC) and N (N_2) in the samples and ultra pure water used for dilution is mandatory. Interferences (see Table 2) need to be carefully assessed and reduced if any. Carbonates, bicarbonates and carbon dioxide as well as all soluble organic materials must be eliminated for carbon SV ICP-MS analysis. For nitrogen SV ICP-MS, nitrate, nitrite and ammonium as well as organic nitrogen compounds must also be eliminated. As an example using the reciprocal of Eq. 2 the signal $s_{^{15}N^+}$ for a 1 ppb N_2 argon - N free sample would be 300 counts for a 1μs Δt (slot time).

For phosphorus and sulphur, all interferences (see Table 3) need to be carefully assessed and reduced if any. A Pt cone is required to avoid any interference from $^{62}Ni^{2+}$ (η_A: 3.6%) with $^{31}P^+$ and $^{64}Ni^{2+}$ (η_A: 0.926%) with $^{32}S^+$. Both could be recorded with the classical nickel cone. Phosphates, phosphites and phosphine as well as organophosphorus (e.g. phosphinites and phosphonites) compounds must be eliminated prior phosphorus SV ICP-MS analysis. Sulphate, sulphites and sulphides as well as sulphurous organic compounds must be absent from the sample prior SV ICP-MS analysis.

The volume of the torch is an issue as well as the size of the cone hole as well as the thermo-hydraulic properties of the plasma (plasma, power source, temperature …). Optimal argon flows, nebulisation and dilution in ultrapure water are a must. Here, the work is carried out for 100 nm viruses using CNPS signals. Interest for other labeling elements such as Se or Na, K, Mg, Ca, Zn and also for smaller viruses should be mentioned. This requires however an improvement of the sensibility e.g. from the pg to the fg level.

To avoid interferences the use of sector field ICP-MS is suggested e.g. Jakubowski *et al* [32]. Work with TOF MS is difficult, quadrupole MSs are better but sector field MSs are strongly recommended to avoid interferences.

Future work concerns the comparison of SV ICP MS scans as calculated for a larger series of viruses with molecular formula $C_\chi H_\eta O_\omega N_\nu P_\pi S_\sigma$ as those given by Popovic & Minceva (2020) [33], for both type (RNA and DNA viruses) and for sizes going from ~20 (if possible) to ~200 nm.

4. Conclusions

This paper is an attempt to review and summarize the different approaches applicable in relation to the detectability in single virus ICP-MS analysis, and highlight the peculiarities of this topic. Interferences are analysed and discussed pointing out the need of SF-ICP-MS.
The analysis of single viruses by SV ICP-MS is possible routinely, recording MS peaks in time scan for given masses and detecting say 2 to 500 viruses in 20 s. The time required for virus counting by SV ICP MS is several thousand time faster than by the other techniques e.g. electron microscopy. Their identification is based on the carbon peak intensity (e.g. $^{13}C^{+}$) which based on the virus molecular weight or mass and the ratio of other master ions (N as surrogate for nucleo-bases and amino acids) and key ions (P as leading element for phosphate from the nucleo-chains, and S for thiol groups) peaks. A virus classification based on the N/C, P/C and S/C molecular ratios is suggested.

Acknowledgements

Acknowledgements are due to Dr Bodo Hattendorf from ETHZ for the constructive discussion we had to optimise the recommendations.

References

[1] C. Degueldre, P.-Y. Favarger, Colloid analysis by single particle inductively coupled plasma-mass spectroscopy: a feasibility study, Coll. Surf. A, 217 (2003) 137-142 . https://doi.org/10.016/S0927-7757(02)00568-X.

[2] C. Degueldre, P. -Y. Favarger,S. Wold, Gold colloid analysis by inductively coupled plasma-mass spectrometry in a single particle mode, Anal. Chim. Acta, 555 (2006) 263-268. https://doi.org/10.1016/j.aca.2005.09.021.

[3] C. Degueldre, P.-Y. Favarger, C. Bitea, Zirconia colloid analysis by single particle inductively coupled plasma–mass spectrometry, Anal. Chim. Acta, 518 (2004) 137-142. https://doi.org/101016/jaca200404015.

[4] C Degueldre, P.-Y Favarger, Thorium colloid analysis by single particle inductively coupled plasma-mass spectrometry, Talanta, 62 (2004) 1051-1054. https://doi.org/ 10.016/j.talanta.2003.10.016.

[5] C Degueldre, P.-Y Favarger, R. Rosé, S. Wold, Uranium colloid analysis by single particle inductively coupled plasma-mass spectrometry, Talanta, 68 (2006) 623-628. https://doi.org/ 10.1016/j.talanta.2005.05.006.

[6] J. Koch, D. Günther, Laser Ablation Inductively Coupled Plasma Mass Spectrometry, Encyclopedia of Spectroscopy and Spectrometry (Third Edition), C (2017) 526-532. https://doi.org/10.1366/11-06255

[7] Ling-Na Zheng, Meng Wang, Bing Wang, Wei-Yue Feng, Determination of quantum dots in single cells by inductively coupled plasma mass spectrometry, Talanta, 116 (2013) 782-787. https://doi.org/ 10.1016/j.talanta.2013.07.075

[8] M. Corte-Rodríguez, R. Álvarez-Fernández, P. García-Cancela, J. Bettmer, Single cell ICP-MS using on line sample introduction systems: Current developments and remaining challenges, TrAC Trends in Analytical Chemistry, 132 (2020) 116042. https://doi.org/10.1016/j.trac.2020.116042

[9] R. S. Amais, G. L. Donati, M. A.Zezzi Arruda, ICP-MS and trace element analysis as tools for better understanding medical conditions, TrAC Trends in Analytical Chemistry, 133 (2020) 116094. https://doi.org/10.1016/j.trac.2020.116094

[10] E. V. Shun'ko, D. E. Stevenson, V. S. Belkin, Inductively Coupling Plasma Reactor With Plasma Electron Energy Controllable in the Range From ~6 to ~100 eV. IEEE, Transactions on Plasma Science. 42 (2014) 774–785. https://doi.org/10.1109/TPS.2014.2299954

[11] E. T. Luong, R.S Houk, Determination of carbon isotope ratios in amino acids, proteins, and oligosaccharides by inductively coupled plasma-mass spectrometry, J. Am. Soc. Mass Spectrom., 14 (2003) 295-301. https://doi.org/10.1016/S1044-0305(03)00003-5.

[12] J.G. Martínez-Sierra, O.G. San Blas, J.M.Marchante Gayón, J.I. García Alonso, Sulfur analysis by inductively coupled plasma-mass spectrometry: A review, Spectrochim. Acta B, (2015) 35-52. https://doi.org/ 10.1016/j.sab.2015.03.016.

[13] S. Faßbender, K. Rodiouchkina, F. Vanhaecke, B. Meermann, Method development for on-line species-specific sulfur isotopic analysis by means of capillary electrophoresis/multicollector ICP-mass spectrometry, Anal. Bioanal. Chem., 412 (2020) 5637–5646. https://doi.org/10.1007/s00216-020-02781-8

[14] F. Laborda, A. C. Gimenez-Ingalaturre, E. Bolea, J. R. Castillo, About detectability and limits of detection in single particle inductively coupled plasma mass spectrometry, Spectrochim. Acta B. 169 (2020) 105883. https://doi.org/10.1016/j.sab.2020.105883

[15] L. A. Rush, C. E. Mackenzie, M. Liezers, A. M. Duffin, Collisional dampening for improved quantification in single particle inductively coupled plasma mass spectrometry, Talanta 189 (2018) 268-273. https://doi.org/10.1016/j.talanta.2018.06.071.

[16] M. Loula, A. Kaňa, O. Mestek, Non-spectral interferences in single-particle ICP-MS analysis: An underestimated phenomenon, Talanta, 202 (2019) 565-571. https://doi.org/10.1016/j.talanta.2019.04.073.

[17] H. Vanhoe, J. Goossens, L. Moens, F.J. Dams, Spectral and non-spectral interferences in inductively-coupled plasma mass-spectrometry**,** Microchim. Acta, 119 (1995) 277-286. https://doi.org/10.1007/BF01244007.

[18] P. Kralj, M. Veber, Investigations into nonspectroscopic effects of organic compounds in inductively coupled plasma mass spectrometry, Acta Chim. Slov., 50 (2003) 633-644. https://doi.org/-

[19] M. Witzler, F. Küllmer, K. Günther, Validating a single-particle ICP-MS method to measure nanoparticles in human whole blood for nanotoxicology, Anal. Lett., 51 (2018) 587-599. https://doi.org/10.1080/00032719.2017.1327538.

[20] Y. Cao, J. Feng, L. Tang, Ch. Yu, G. Mo, B. Deng, A highly efficient introduction system for single cell- ICP-MS and its application to detection of copper in single human red blood cells, Talanta, 206 (2020) 120174. https://doi.org/10.1016/j.talanta.2019.120174

[21] R. E. F. Matthews, A Classification of Virus Groups Based on the Size of the Particle in Relation to Genome Size, J. Gen. Virol. 27 (I975) 135-149. https://doi.org/10.1099/0022-1317-27-2-135.

[22] A. K. Shanker, D. Bhanu, A. Alluri,' S. Gupta, Whole-genome sequence analysis and homology modelling of the main protease and non-structural protein 3 of SARS-CoV-2 reveal an aza-peptide and a lead inhibitor with possible antiviral properties, New J. Chem. 44 (2020) 9202-9212 https://doi.org/10.1039/D0NJ00974A

[23] J.C. Hierholzer, E.L. Palmer, S.G. Whitfield, H.S. Kaye, W.R. Dowdle, Protein composition of coronavirus OC 43, Virology, 48 (1972) 516-527. https://doi.org/10.1016/0042-6822(72)90062-1.

[24] B. G. Hogue, D. A. Brian, Structural proteins of human respiratory coronavirus OC43, Virus Res., 5 (1986) 131-144. https://doi.org/10.1016/0168-1702(86)90013-4

[25] M. Popovic, M. Minceva, Thermodynamic insight into viral infections 2: empirical formulas, molecular compositions and thermodynamic properties of SARS, MERS and SARS-CoV-2 (COVID-19) viruses, Heliyon, 6 (2020) e04943. https://doi.org/10.1016/j.heliyon.2020.e04943.

[26] B.W. Neuman, G. Kiss, A.H. Kunding, D. Bhella, M.F. Baksh, S. Connelly, B. Droese, J.P. Klaus, S. Makino, S.G. Sawicki, S.G. Siddell, D.G. Stamou, I.A. Wilson, P. Kuhn, M.J. Buchmeier, A structural analysis of M protein in coronavirus assembly and morphology, J. Struct. Biol., 174 (2011) 11-22. https://doi.org/1016/j.jsb.2010.11.021.

[27] B.W. Neuman, B.D. Adair, C. Yoshioka, J.D. Quispe, G. Orca, P. Kuhn, R.A. Milligan, M. Yeager, M.J. Buchmeier, Supramolecular architecture of severe acute respiratory syndrome coronavirus revealed by electron cryomicroscopy, J. Virol., 80 (2006) 7918-7928 https://doi.org/10.1128/JVI.00645-06

[28] C.D. Humphrey, Negative stain electron microscopy shows a SARS-CoV particle with club-shaped surface projections surrounding the periphery of the particle, a characteristic feature of coronaviruses. Centers for Disease Control and Prevention, Image Library (2021). https://www.cdc.gov/media/subtopic/images.htm

[29] Z.-M. Wang, R. Ma, R.N. Pierson, S.B. Heymsfield, Five level model: reconstruction of body weight at atomic, molecular, cellular, and tissue-system levels from neutron activation analysis, K.J. Ellis, J.D. Eastman (Eds.), Human Body Composition, Plenum Press, New York (1993), pp. 125-128. https://doi.org/10.1007/978-1-4899-1268-8_28

[30] S. Domingez-Medina, S. Forstner, M. Deffrt, M. Sansa, A-K. Stark, M.A. Halim, E. Vernhes, M. Gely, G. Jourdan, T. Alava, P. Boulanger, Ch. Masselon, S. Hentz, Neutral mass spectrometry of virus capsids above 100 megadaltons with nanomechanical resonators, Sci. 362 (2018) 918-922. https://doi.org/10.1126/science.aat6457

[31] M. Riisom, B. Gammelgaard, I.H. Lambert, S. Stürup, Development and validation of an ICP-MS method for quantification of total carbon and platinum in cell sample and comparison of open vessel and microwave assisted acid digestion methods, J. Pharma. Biomed. Anal., 158 (2018) 144-150. https://doi.org/10.1016/j.jpba.2018.05.038.

[32] N. Jakubowski, L. Moens, F. Vanhoecke, Sector field mass spectrometer in ICP-MS, Spectrochim. Acta B 53 (1998) 1739-1763. https://doi.org/10.1016/S0584-8547

[33] M. Popovic, M. Minceva, Thermodynamic insight into viral infections: do viruses in a lytic cycle hijack cell metabolism due to their Gibbs energy?, Heliyon, 6 (2020) e03933. https://doi.org/10.1016/j.heliyon.2020.e03933

Click here to access/download;Figure;SV ICP MS paper 06 12 2020 Fig1.doc

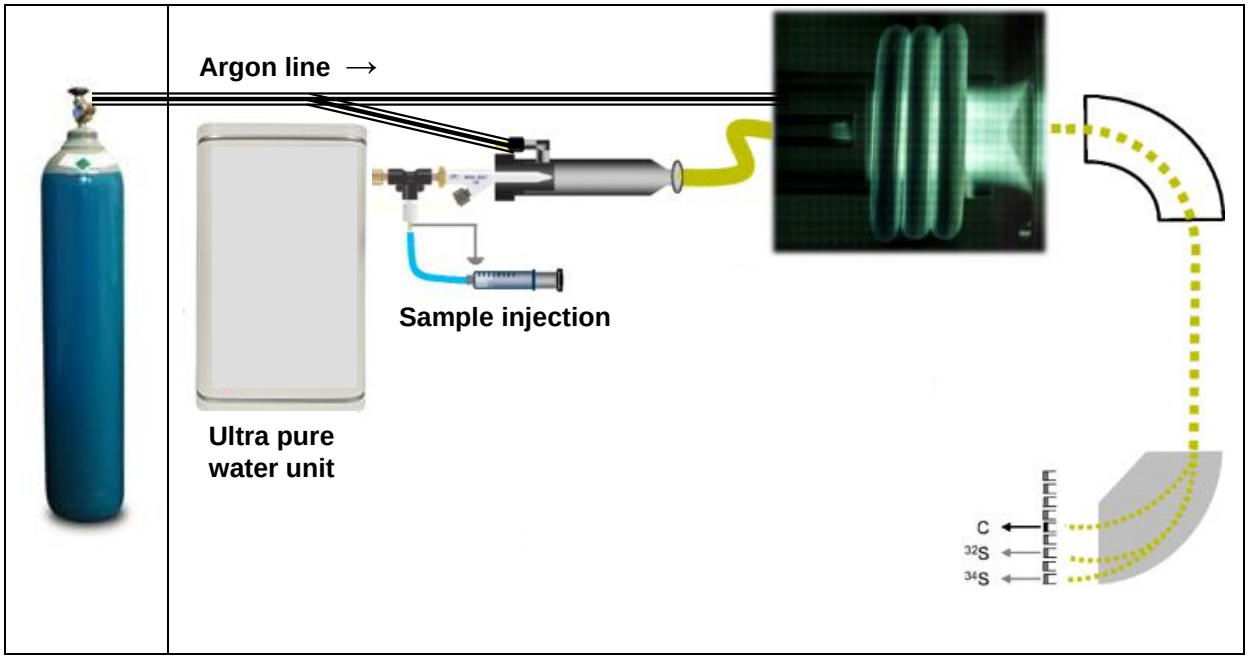

Fig. 1: Single Virus Multi-Channel Inductively Coupled Plasma Mass Spectrometry SV MC ICP MS adapted for master ions and key ions analysis. Note the dilution factor used when injecting the sample (syringe) in the stream of pure water, see Degueldre & Favarger (2003).

Click here to access/download;Figure;SV ICP MS paper 06 12 2020 Fig2.doc

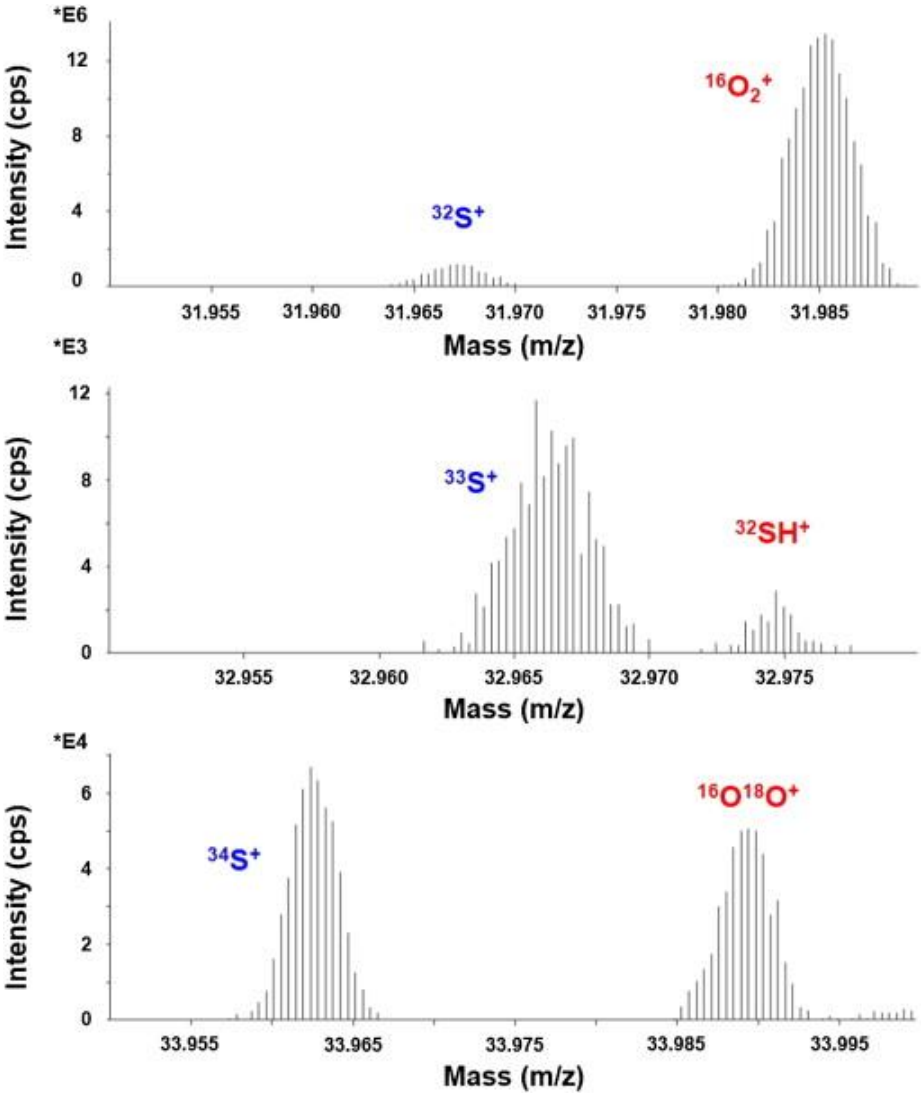

Fig. 2: Discriminating $^{A}S^{+}$ and their interferences by HR MC ICPMS Ref. Martínez-Sierra, *et al* (2015).

Click here to access/download;Figure;SV ICP MS paper 07 02 2021 Fig3.doc

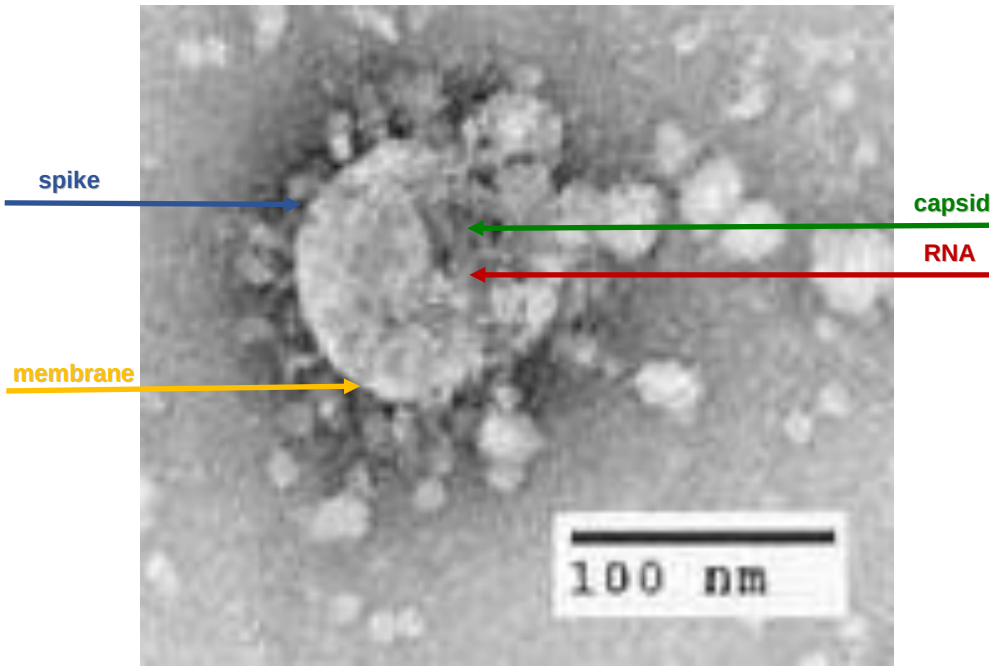

Fig. 3: Negative stain electron microscopy SARS-COV 2 showing spikes, membrane, capsid and RNA genome. Adapted from Humphrey [28].

Click here to access/download;Figure;SV ICP MS paper 06 12 2020 Fig4.doc

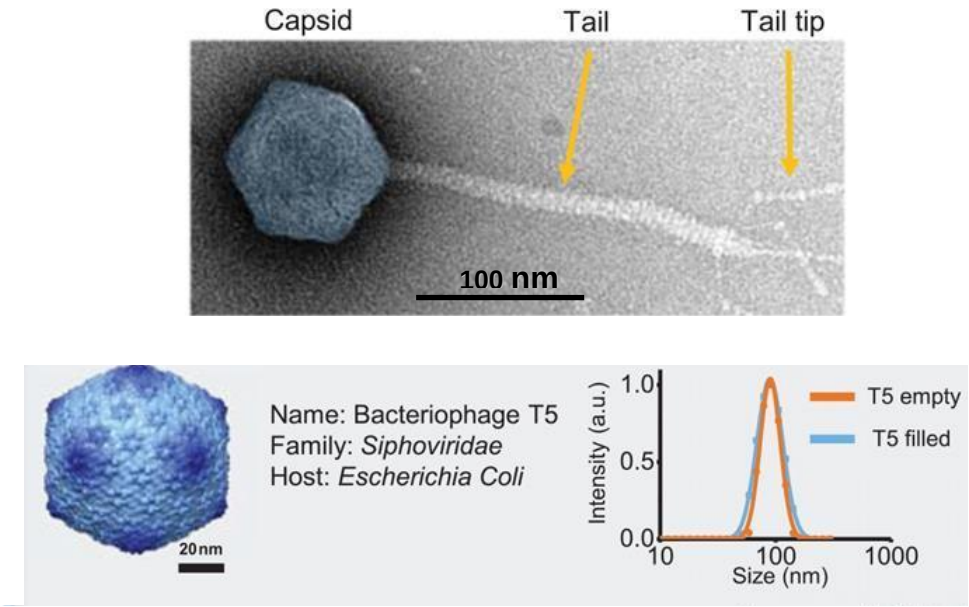

Fig. 4: Morphological characteristics of the Siphoviridae T5 bacteriophage virus. Chemical composition, see **Table 6**

Click here to access/download;Figure;SV ICP MS paper 06 12 2020 Fig5.doc

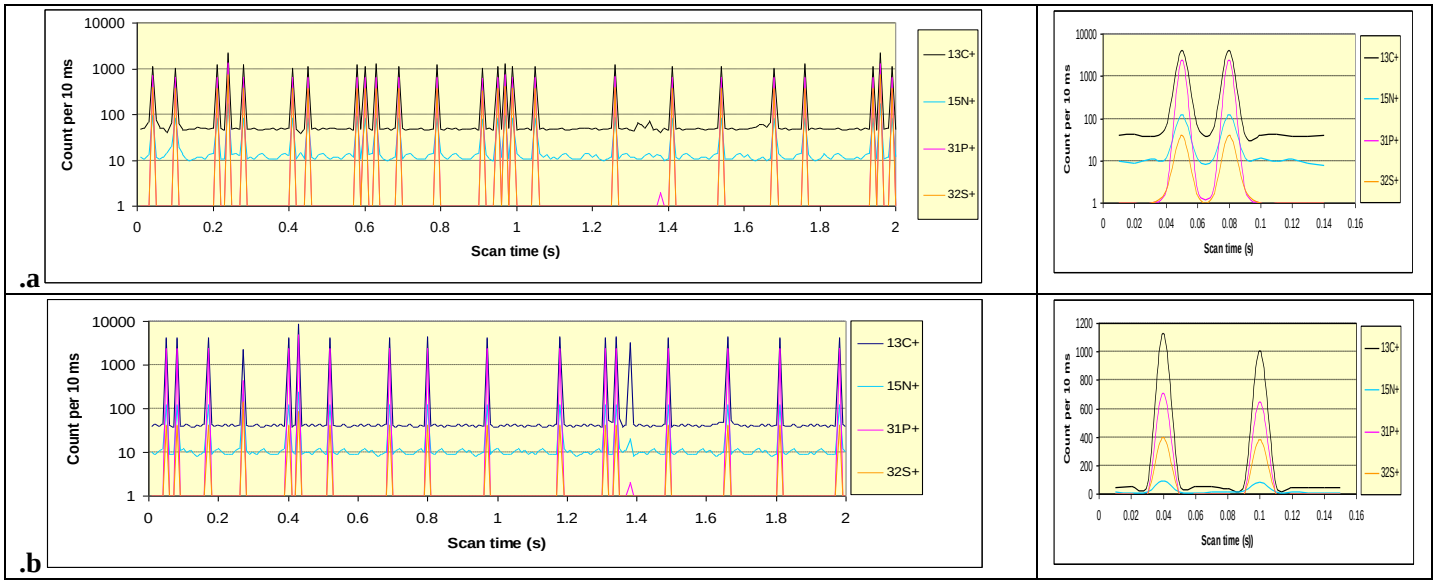

Fig. 5: Simulated SV ICP MS scan for analysis of Viruses.
a. 24 single SARS COV-2 viruses +2 counted as double
b. 16 single sipho-viridae T5 bacteriophage viruses +1 counted as double.
Conditions: recording time 2 s, Δt: 10 ms, η_C : $2x10^{-2}$, η_A: $^{13}C^+$: 1.10%, $^{15}N^+$: 0.366%, $^{31}P^+$: 100%, $^{32}S^+$: 95%, other conditions see Table 1. Readings: **a.** at 0.26 s and 1.95 s: aggregates of 2 viruses, 1.38 bio-fragment e.g. cellulose nano particle, **b**. at 0.42 s: aggregate of 2 viruses, for **a.** & **b.** the $^{13}C^+$ background is due to residual DOC and traces of CO_2, the $^{15}N^+$ background is due to residual dissolved N_2 in solution and traces of N in DOC.

Cover letter

Professor
Claude Degueldre
Engineering Department,
Lancaster University,
Lancaster LA1 4YW, UK

Dec. 06, 2020

To the Editor
Talanta
Elsevier

Because of the urgency nature of this manuscript topic I thank you to give high priority for the handling of this work.

Dear Editor,

We are pleased to submit our manuscript:
Single virus inductively coupled plasma mass spectroscopy analysis: a comprehensive study
By Claude Degueldre
for publication in Talanta.

This study suggests to adapting this method for single viruses (SV) identification and counting. With multi-channel ICP-MS records in SV detection mode, the counting of master and key ions can allow analysis and identification of single viruses. The counting of 2-500 virial units can be performed in 20 s.
Application for two virus types (SARS-COV2 and T5 sipho bacteriophage) is investigated using time scan and fixed mass analysis for the selected virus ions allowing characterisation of the species using the N/C, P/C and S/C molar ratio's
These points make the manuscript of great interest for the readers of Talanta.

We look forward to hearing from you soon.

With my best regards,

Professor Dr Claude Degueldre
Engineering Department,
Lancaster University, UK

Novelty statements

This is the first time the time scan of single virus (SV) ICP MS is presented. It is modelled for several elements which are master and key element or a virus. There reading allow evaluation of the virus concentration number per viridae families based on the peaks ratio N/C, P/C and S/C…

The counting can be of 2 to 500 viruses in 20 s.

Check list

1. Cover letter
2. Novelty statement
3. Highlights
4. Graphical abstract
5. Manuscript
6. Fig1
7. Fig2
8. Fig3
9. Fig4
10. Fig5
11. Check list
12. Potential reviewers
13. Declaration interest

Reviewers SV ICP-MS paper

Professor Marco A. Zezzi Arruda
Spectrometry, Sample Preparation and Mechanization Group (GEPAM), Institute of Chemistry, University of Campinas, PO Box 6154, Campinas, SP, 13083-970, Brazil
zezzi@unicamp.br
Professor Titular, Departamento de Química Analítica, Instituto de Química, Universidade de **Campinas** – Unicamp trace analysis by ICPMs application for medical issues

Dr Marko Popovic
marko.popovic@tum.de
Biothermodynamics, TUM School of Life Sciences Weihenstephan, Technical University of Munich, Maximus-von-Imhof-Forum 2, 85354, Freising, Germany
Researcher,

Professor Dr Benedikt B. Kaufer
Institute of Virology, Freie Universität Berlin, Berlin, Germany
Corresponding authors:
b.kaufer@fu-berlin.de
Viral Integration, Tumorigenesis and Virus Evolution

Professor Dr Jorg Bettmer
bettmerjorg@uniovi.es
University of Oviedo, Department of Physical and Analytical Chemistry, Faculty of Chemistry and Instituto de Investigación Sanitaria del Principado de Asturias (ISPA), C/ Julián Clavería 8, E-33006, Oviedo, Spain
Expert in SP ICPMS

Pr Dr Detlef Günther
ETH Zurich, Laboratory of Inorganic Chemistry, Wolfgang-Pauli-Strasse 10, 8093 Zurich, Switzerland
Corresponding author at: ETH Zurich, Laboratory of Inorganic Chemistry, HCI G113, Wolfgang-Pauli-Strasse 10, 8093 Zurich, Switzerland. Tel.: +41 44 632 4687; fax: +41 44 633 1071.
guenther@inorg.chem.ethz.ch
Expert in ICPMS

Declaration of interests

☒ The authors declare that they have no known competing financial interests or personal relationships that could have appeared to influence the work reported in this paper.

☐The authors declare the following financial interests/personal relationships which may be considered as potential competing interests:

SV ICPMS author credit
TAL-D-20-04072

The authors was not supported for this study…

For safety reason please send also copy of mails to degueldreclaude@gmail.com

Single virus inductively coupled plasma mass spectroscopy analysis: a comprehensive study.

Claude Degueldre
Engineering Department, Lancaster University, Lancaster LA1 4YW, UK
c.degueldre@lancaster.ac.uk

Abstract
The characterisation of individual nanoparticles by single particle ICP-MS (SP-ICP-MS) has paved the way for the analysis of smallest biological systems. This study suggests to adapting this method for single viruses (SV) identification and counting. With high resolution multi-channel sector field (MC SF) ICP-MS records in SV detection mode, the counting of master and key ions can allow analysis and identification of single viruses. The counting of 2-500 virial units can be performed in 20 s. Analyses are proposed to be carried out in Ar torch for master ions: $^{12}C^+$, $^{13}C^+$, $^{14}N^+$, $^{15}N^+$, and key ions $^{31}P^+$, $^{32}S^+$, $^{33}S^+$ and $^{34}S^+$. All interferences are discussed in detail. The use of high resolution SF ICP-MS is recommended while options with anaerobic/aerobic atmospheres are explored to upgrade the analysis when using quadrupole ICP-MS. Application for two virus types (SARS-COV2 and bacteriophage T5) is investigated using time scan and fixed mass analysis for the selected virus ions allowing characterisation of the species using the N/C, P/C and S/C molar ratio's and quantification of their number concentration.

Keywords: Virus identification; virus counting; SP ICP-MS; individual virus analysis; single virus ICP-MS.

1. Introduction

Single particle inductively coupled plasma mass spectroscopy (SP ICP-MS) was first tested at Institute Forel, University of Geneva in 2001 and presented in 2002 at the EMRS Spring Meeting in a proceedings paper published by Degueldre & Favarger (2003)[1]. This method was later tested on gold nano- particles that are used as substrate in nano- pharmacy, and published subsequently i.e. Degueldre *et al* (2006)[2]. SP ICP-MS was also tested on dioxides e.g. Degueldre *et al* (2004 & 2006)[3,4,5]. The characterisation of individual metallic nanoparticles by ICP-MS analysis has been carried out by laser ablation as reviewed by Koch & Günther (2017)[6] or by so-called single particle ICP-MS which has paved the way for the analysis of small biological systems like individual microscopic cells e.g. Zheng *et al* (2013)[7] and Corte-Rodríguez *et al* (2020)[8]. Today the challenge of very sensitive ICP-MS methods is to solve specific medical issues such as contaminations pathways or viruses spreading and the role of forgotten elements e.g. Te as pointed out by Amais *et al* (2020)[9]. This conceptual study suggests the use this method for single viruses (SV) ICP-MS identification and counting. Its potential is tested for two virus kinds: one of RNA and one of DNA type.

2. Methodology

To perform SV ICP-MS high dilution of the viral sample suspension is required to inject one virus at a time in the plasma torch, producing one flash of ions per slot time of the Mass Spectrometer. After atomisation/ionisation in the plasma torch the flash of ion (cloud) passes through the conus pin hole and is analysed in the mass spectrometer. The number of flash is proportional to the concentration of viruses in the sample, and the intensity of the ionic flash is proportional to the fraction of the element (isotope ion) present in the viral object. For practical reason one considers the argon (Ar) plasma torch.

In nanomedicine virus analysis is a key issue, however current molecular analysis is usually time consuming. In this study for virus identification one is interested to discriminate the fraction of master ions (atoms from the matrix of the virus) and the fraction of key element (ion from a coating e.g. drug, or from a selected element e.g. specific for given amino acid or for the viral RNA or DNA). In the case of a given virus, for example, SV ICP-MS shall require the selection of one (or two) master ion(s) and of 2 key ions to identify them and quantify their fraction in the virus 'body'.

In ICP-MS analyses the introduced sample is largely ionized in the plasma followed by a separation of the ions by their mass-to-charge ratio. A resulting ion beam is then quantified via calibration of the associated signal intensities. Usually the argon plasma is operated under atmospheric conditions and the analytes are transported there either in acidified (or basic) aqueous solution or in organic solvents, the most abundant elements in the plasma next to Ar are H, O, N, and C. To reduce contamination (C,N,O) the torch is placed in argon atmosphere. **Table 1** provides standards experimental conditions to perform SP ICPMS analysis.

Table 1 Typical Instrument and operating conditions for ICP-MS

Radio frequency applied power (kW)	1.4
Plasma gas flow rate (L min^{-1})	18.0
Nebulizer gas flow rate q_{neb} / (L min^{-1})	1.0
Auxiliary gas flow rate / (L min^{-1})	1.8
Sheath gas flow rate / (L min^{-1})	0.13
Sampling depth / (mm)	5.5
Ultra pure water flow rate (mL min^{-1})	200
Sample injection flow rate (mL min^{-1})	0.20
Replicates *per* sample	5
Spray chamber temperature / (ºC)	2
Mass-to-charge ratio (*m/z*) master ions	12, 13, 14, 15, ,

Mass-to-charge ratio (*m/z*) key ions	31, 32, 34,
Scan mode	Time
Acquisition mode	Multi-channel, fixed masses, time-scan

Since the quadrupoles can be tuned to select for different masses, they are ideally suited for the interferences. The first mass filter is then set to the analyte plus its interference, e.g. m/z 32 for sulphur, after the reaction cell e.g. A+1 with H of H_2 and A+16 with O of O_2.

A little intensity is lost through the process, but the gain is worth the loss: interference being drastically lowered, the collision/reaction cell's performance is at its best level. The advantages and disadvantages of ICP-MS is its very large range of analysis, however SV ICP-MS remains a non-species selective analysis.

On the other hand, in a known matrix with a known analyte, a very accurate quantitation can be performed by the mean of a conversion factor for calculation of the species of interest. If a soluble or gaseous interferes in the scan signal (background), it can be reduced by dilution in the stream of pure water used in SV mode. The advantage of this method is the principle of analysis itself that gets rid of organic compounds that could interfere in other types of measurements by a digestion step (solid samples) and/or directly by the subsequent plasma ionization.

Multi-Channel (MC) ICP-MS allows, compared to simple quadrupole ICPMS, a finer analysis due to the addition of a supplementary quadrupole to the system before the collision / reaction cell. This addition acts as a supplementary mass filtering unit thus removing more of the interferences. Use of a sector field (SF) improves also widely the technique (better resolution, multi -channel analysis).

Since today's sector field MC ICP-MS (see **Fig. 1**) can detect some atoms (say 5-20 ions per ion flash and per channel) the potential of this technique is impressive. However, a full analysis of the potential interfering ions is mandatory.

Fig. 1: Single Virus Multi-Channel Inductively Coupled Plasma Mass Spectrometry SV MC ICP MS adapted for master ions and key ions analysis. Note the dilution factor used when injecting the sample (syringe) in the stream of pure water, see Degueldre & Favarger (2003).

2.1 Virus master ion analysis

The virus major ions are those ions from the main elements of the virus in the membrane, S-protein, lipid layers, capsid as well as in the nucleic (RNA or DNA) core. These elements are H, C, N and O. For the mass spectrometer of the ICP-MS, ion isotopes detected shall be $^{12}C^+$, $^{13}C^+$, $^{14}N^+$, $^{15}N^+$. They are reported in **Table 2** with their potential interferences in the Ar plasma. H and O isotopes are not considered because they are due to water itself from the solution and from the hydration of the viral object. Note that the dissolved (and the low molecular suspension) molecules appear in the MS reading as a continuum and that the SV and SP signals are ion peaks. Interferences on $^{A}X^+$ are easy to sort out; they are $[^{A/2}X'_2]^+$, $[^1H^{A-1}X']^+$, $[^1H_2{}^{A-2}X']^+$, $^{nA}X'^{n+}$, where X' is the interfering element isotope of mass derived from ^{A}. Potential interferences are reported in **Table 2**. Their masses give their potential of interference on the mass scale and their abundances guide the overlapping effect they may have in the intensity scale.

2.1.1 Measuring carbon

For $^{12}C^+$ the interferences (given in **Table 2**) may be: $[^6Li_2]^+$, $[^1H^{11}B]^+$, $^{24}Mg^{2+}$and $^{48}Ti^{4+}$, however these elements may be absents or very diluted in the suspension. Only $^{36}Ar^{3+}$ could interfere, however its abundancy is 0.337% in Ar reducing its impact and its triple ionisation may be avoided at lower plasma temperature which are usually several orders of magnitude greater than the temperature of the neutral species, see Shun'ko *et al* (2014)[10]. With a mass difference of 0.007 $^{24}Mg^{2+}$ may interfere with $^{12}C^+$, however, dilution is possible when Mg is soluble. Otherwise the reaction cell described below for $^{13}C^+$ is applicable.

For $^{13}C^+$ the interferences (given in **Table 2**) may be: $[^1H^{12}C]^+$, $[^2H^{11}B]^+$, $^{26}Mg^{2+}$ and $^{39}K^{3+}$. The solution must be exempted of B, Mg and K. If one of these ions interferes as soluble it may be further diluted to reduce the background without affecting the height of the single particle peaks. Decreasing slightly the flow rate of the aerosol gas from that which yields maximum signal eliminates this $^{12}C^1H^+$ interference as reported by Luong & Houk (2003)[11]. Additional information is given in **Table 2**. Clearly with a mass difference of 0.005 $[^1H^{12}C]^+$ may interfere with $^{13}C^+$. For oxide-forming analytes, this can be achieved elegantly in a reaction cell by the means of oxygen. This interference may be avoided by forming $^{13}C^{16}O^+$ using the reaction:

$^{13}C^+ + {}^{16}O_2 \rightarrow {}^{13}C^{16}O^+ + {}^{16}O$

Actually, the formation of $^{28}Si^+$ from the quartz vessel may interfere on $^{12}C^{16}O^+$ as well as the formation of $^{30}Si^+$ (low abundance) could interfere on $[^1H^{13}C^{16}O]^+$ (low probability of formation). Consequently the use of SF ICP-MS may be suggested.

2.1.2 Measuring nitrogen

For $^{14}N^+$ the interferences may be: $[^7Li_2]^+$, $[^2H^{12}C]^+$ and $^{28}Si^{2+}$. Basically lithium should be in the soluble phase and dilution shall reduce the effect, $^1H_2{}^{12}C$ may be originating from the soluble and particulate (virus) phase and Si could also be part of the soluble phase (soluble SiO_2 or silicates) or from the particle phase e.g. quartz fragments or from the torch. Ultra-traces of N_2 in the carrier gas is also an issue (see discussion). Details are given in Table 2.

For $^{15}N^+$ the interferences may be: $[^1H^{14}N]^+$, $^{30}Si^{2+}$ and $^{60}Ni^{4+}$. Basically HN may be originating from the soluble and particulate (virus) phase and Si could also be part of the soluble phase (soluble SiO_2 or silicates) or from the particle phase e.g. quartz fragments from the nebuliser/torch vessel. Details are given in Table 2. Here the mass differences (N^+ and interference) are larger than 0.008 and the use of high resolution MS is suggested.

Table 2: Master ion isotopes and their interferences considered for the SV ICP-MS analysis. Molecular mass $\mathcal{M}(^A[X]^+)$ of $^A[X]^+$ and its abundance: Abd.

Isotope ^AX	$\mathcal{M}(^A[X]^+)$	Abd (%)	Interference	$\mathcal{M}(^A[YZ]^+)$, $\mathcal{M}(^{nA}[Y]^{n+})$	Abd (%)
^{12}C	11.99945	98.900	$[^1H^{11}B]^+$,	12.01659	80.09
			$^{24}Mg^{2+}$,	11.99252	62.39
			$^{36}Ar^{3+}$,	11.98863	00.337
			$^{48}Ti^{4+}$,	11.98644	73.8
^{13}C	13.00280	01.100	$[^1H^{12}C]^+$,	13.00728	98.885
			$^{26}Mg^{2+}$,	12.99075	11.01
			$^{39}K^{3+}$,	12.98735	93.258
^{14}N	14.00252	99.634	$[^1H^{13}C]^+$,	14.01008	01.998

			$^{28}Si^{2+}$,	13.98702	92.23
^{15}N	14.99956	00.366	$[^{1}H^{14}N]^{+}$,	15,01063	99.619
			$^{30}Si^{2+}$,	14.98634	03.10
			$^{60}Ni^{4+}$,	59.930785	26.223

All these interferences may also be avoided using high resolution MS.

2.2 Virus key ion analysis

The virus key ions are those from these elements that characterise its properties and functionalities. **Phosphorus** is an integral part of the nucleotides and thus of all fragments of DNA and RNA, so it can be used to quantify such macromolecules. **Sulphur** is present in large molecules, either as active groups, e.g. in thiols, or within the normal structure of specific amino acids. In SV analysis it is consequently essential to quantify the elemental fractions of these elements.

The key ion isotopes are subject like major element to interferences. The more relevant isobaric interferences are given in **Table 3**. Interferences on $^{A}X^{+}$ are easy to evaluate; these are $[^{A/2}X'_2]^{+}$, $[^{1}H^{A-1}X']^{+}$, $[^{1}H_2{}^{A-2}X']^{+}$, $^{nA}X'^{n+}$, but also $[^{16}O^{A-16}X']^{+}$ and $[^{16}O_2{}^{A-32}X']^{+}$.

The low mass-range of the ICP-MS is very "crowded" by $[NO]^{+}$, $[O_2]^{+}$, $[CO]^{+}$, varying in their mass by the combination and abundance of their respective fractions. For example, $[^{16}O_2]^{+}$ with the mass 32 is very common, and while $[^{15}O_2]^{+}$ with 30 is much less abundant, $[^{14}N^{16}O]^{+}$ also contributes at this mass. In case the mass of interest is affected by such polyatomic interferences, an effective way to solve the interference is needed. The solution is to work in a He atmosphere surrounding the Ar torch system avoiding the N_2, O_2 and CO_2 contamination of the system. Some of these cluster ions may interfere with the measured key ions $^{31}P^{+}$, $^{32}S^{+}$ and $^{33}S^{+}$.

2.2.1 Measuring phosphorus

Phosphorus is a mono-isotopic element of mass 30.97 amu. For a mass-based analytical technique like ICP-MS, this means that only the one isotope (^{31}P) can be selected to quantify phosphorus. **For $^{31}P^{+}$** the interferences are given in **Table 3**.

The phosphorus analysis by ICP-MS is somewhat limited by a weak detection limit, as reviewed by Martínez-Sierra, *et al* (2015)[12]. Since their detection limit is weak in current argon plasma troch a variant is mandatory. Measuring option is to use the ICP-MS - O_2 reaction cell to analyse phosphorus.

For phosphorus, which receives strong interference from multiple ions (like $[^{15}N^{16}O]^{+}$, $[^{1}H^{14}N^{16}O]^{+}$, $[^{13}C^{18}O]^{+}$, ...) or $^{62}Ni^{2+}$ see Table 3, a solution may be a mass shift from 31 to 47 amu with:

$$^{31}P^{+} + {}^{16}O_2 \rightarrow [^{31}P^{16}O]^{+} + {}^{16}O$$

For the interfering species, mass remains 31 amu:

$$[^{15}N^{16}O]^{+} + O_2 \rightarrow \text{no reaction}$$

However, it must be kept in mind that although the analyte can then be analyzed at a mass different to its interfering species, the mass it is shifted to could be already be "occupied" by other analytes also present in the sample, e.g. ^{47}Ti in the case of $[^{31}P^{16}O]^{+}$. In such cases, with a normal single quadrupole ICP-MS system, one would end up with the same problem, just at another mass.

Interferences may also be avoided using high resolution MS.

2.2.2 Measuring sulphur

The phosphorus and sulfur analysis by ICP-MS is somewhat limited by a weak detection limit, as reviewed by Martínez-Sierra, *et al* (2015). A method for the analysis on-line of species-specific sulfur isotopes by means of multi-collector ICP-mass spectrometry has been proposed by Faßbender, *et al* (2020)[13]. Since their detection limit is weak in current argon plasma troch a variant is mandatory. Measuring option is to use the ICP-MS – O_2 reaction cell to analyse sulphur.

For sulphur, three naturally stable isotopes (^{32}S, ^{33}S, ^{34}S) are found with an abundance of approximately 95% for ^{32}S. For the determination of trace concentrations, the only reasonable isotope is offered by ^{32}S. Their high resolution mass spectra are presented **Fig 2**. For sulfur, which receives strong interference from the ion $[^{16}O_2]^+$ as well as $[^{1}H^{31}P]^+$, $^{64}Zn^{2+}$, $^{96}Mo^{3+}$, and $^{64}Ni^{2+}$ (the later if Zn, Mo or Ni (cone) are present) a mass shift from 32 to 48 amu is suggested using a reaction cell:

$$^{32}S^+ + {}^{16}O_2 \rightarrow {}^{32}S^{16}O^+ + {}^{16}O$$

While the interfering ion mass remains 32 amu for $^{16}O_2$.
However, it must be kept in mind that although the analyte can then be analyzed at a mass different to its interfering species, the mass it is shifted to could be already be "occupied" by other analytes also present in the sample, e.g. $^{48}Ti^+$ in the case of $[^{32}S^{16}O]^+$. In such cases, with a normal single quadrupole ICP-MS system, one would end up with the same problem, just at another mass. Interferences may also be avoided using high resolution MS.

Table 3: Key ion isotopes considered for the SV ICP-MS analysis. Molecular mass $\mathcal{M}({}^{A}[X]^{+})$ of ${}^{A}[X]^{+}$ and its abundance Abd.

Isotope ${}^{A}X$	$\mathcal{M}({}^{A}[X]^{+})$	Abd (%)	Interference	$\mathcal{M}({}^{A}[YZ]^{+})$, $\mathcal{M}({}^{2A}[Y]^{2+})$	Abd (%)
${}^{31}P$	30.97321	100.000	$[{}^{15}N{}^{16}O]^{+}$	30.9945	00.365
			$[{}^{1}H{}^{14}N{}^{16}O]^{+}$	31.0091	99.382
			$[{}^{13}C{}^{18}O]^{+}$	31.0026	00.022
			${}^{62}Ni^{2+}$	30.9642	03.634
${}^{32}S$	31.97152	95.02	$[{}^{1}H{}^{31}P]^{+}$,	31.98104	99.985
			${}^{64}Zn^{2+}$,	31.96402	48.60
			$[{}^{16}O_2]^{+}$	31.98927	99.525
			${}^{64}Ni^{2+}$	31.9640	00.926
${}^{33}S$	32.97091	0.75	$[{}^{1}H{}^{32}S]^{+}$	32.97935	95.006
${}^{34}S$	33.96732	4.21	$[{}^{16}O{}^{18}O]^{+}$	33.99352	00.199

Fig. 2: Discriminating ${}^{A}S^{+}$ and their interferences by HR MC ICPMS Ref. Martínez-Sierra, *et al* (2015).

Un-labelled virus identification may consequently be done by measuring master ions and the key ions. The first give a weight of carbon, nitrogen and oxygen and could be used to derive a total mass (in Da) of the virus, on the basis of calibration. The oxygen data may be affected by the virus hydration grade. The key ion data allow by deduction identification of the virus based on its functionalities derived from specific amino acids present in the virus. In all case the concentration of the virus (in number per mL) can be deduced.

3. Application and discussion

3.1 Application of the single particle methodology

Single particle inductively coupled plasma mass spectrometry (SP-ICP-MS) offers unique features for the detection of particles, as well as for their quantification and size characterization. The detection capabilities of SP-ICP-MS are therefore not only limited to the concentration domains (of particles and dissolved related species), but also to the mass of element per particle and particle size domains as reported by Degueldre & Faverger (2003) and confirmed by Laborda *et al* (2020)[14]. Discrimination and detection of particle events, based on the use of robust limits of decision and the estimation of the limits of detection in the different domains, require standardized metrological approaches that have not been clearly established yet. As a consequence, harmonized approaches and expressions to allow reliable comparisons between methods and instruments, as well as to process SP-ICP-MS data, are required.

ICP-MS is a powerful method, unfortunately, the linear dynamic range of single particle analysis may be hindered by "unruly" transient signals and momentary pulse pile-ups at the electron multiplier detector see Rush *et al* (2018)[15]. This study investigated a way to extend the dynamic range of ICP-MS nano-particle quantification *via* addition of a collision gas in the collision cell of the ICP-MS. The collision gas temporally broadens the nano-particle

signal resulting in decreased pulse pile-up and increased integrated intensity, up to a point where scattering losses begin to dominate. The addition of a collision gas used together with the dual mode detector shows a promising path forward towards mitigating unruly transient signals, improving the dynamic range of nano-particle quantification.

Non-spectral interferences in single-particle ICP-MS analysis is another underestimated phenomenon according to Loula *et al* (2019)[16]. Spectral and non-spectral interferences in inductively-coupled plasma mass-spectrometry were investigated by Dams *et al* (1995)[17]. Non-spectroscopic effects of organic compounds were also investigated by Kralj & Veber (2003)[18].

Single-particle ICP-MS method was validated by Witzler *et al* (2018)[19] to measure nano-particles in human whole blood for nano-toxicology. A highly efficient introduction system for single cell- ICP-MS and its application to detection of copper in single human red blood cells has been reported by Cao *et al* (2019)[20].

The number of X ions N_X (-) for a single virus $C_\chi H_\eta O_\omega N_\nu P_\pi S_\sigma$ (with ξ: χ, η, ω, ν, π, and σ the stoichiometric coefficient of X: C, H, O, N, P or S) of size d_{vir} (cm) is given by:

$$\xi = N_X = \frac{\xi \pi d_{vir}^3 \rho N_{Av}}{6 M(vir)} \quad (1)$$

where ρ (g cm^{-3}) is the virus density, N_{Av} the Avogadro constant (mol^{-1}), the virus molecular weight $\mathcal{M}_{(C_\chi H_\eta O_\omega N_\nu P_\pi S_\sigma)}$ (simplified as M(vir)).

The number of atoms N_X is also deduced from the signal $s_A(t)$ during its appearance (between t_1 and $t_1+\Delta t$, with Δt the full peak time) by the expression:

$$N_X = \frac{1}{\eta_A \eta_C} \int_{t_i}^{t_i+\Delta t} s_A(t)\, dt \quad (2)$$

With η_A for ^{A}M the isotopic abundance and η_c the counting efficiency.
The virus number concentration N_{vir} (ml^{-1}) in the original suspension is diluted by a factor q_{vir}/q_{sol}. The fraction η_{neb} is found in argon, which mass flow is q_{Ar}. The dilution is only valid for the dissolved species. However, the virus as single entity remains entire and is not diluted. Its appearance frequency $f(s_A)$ (s^{-1}) of virus ion flashes in the torch is given by:

$$f(s_A) = N_{vir}\ q_{vir}\ \eta_{neb} \quad (3)$$

These equations allow evaluation of the size distribution for a given element/isotope in the virus phase to be evaluated.

Now the SV-ICP-MS method has a very powerful potential with the possibility to analyze 2 to 500 viral objects in 20 s which can be explored for 2 kinds of viruses as examples.

3.2 Single virus data analysis

A virus is a composite object that may be characterized by its chemical composition, which chemical formula reads:

$$C_\chi H_\eta O_\omega N_\nu P_\pi S_\sigma,$$

with χ, η, ω, ν, π, and σ the stoichiometric coefficient of C, H, O, N, P and S respectively. In SV analysis it is essential to quantify the elemental fractions of these elements. They are

constituents of specific amino acids, some of which are reported in Table 4. These are the constituents of proteins.

The molecular weight of the virus M(vir) is calculated as:

$$M(vir) = \chi\, \mathcal{M}(C) + \eta\, \mathcal{M}(H) + \omega\, \mathcal{M}(O) + \nu\, \mathcal{M}(N) + \pi\, \mathcal{M}(P) + \sigma \mathcal{M}(S) \quad (4)$$

It may be evaluated from the mass of fragments and their composition of these virus parts. Their chemical composition is estimated within a variation that can be of the order of easily 10%. Table 4 gives some key components of living mater.

The SV ICP MS time scan can be recorded and analysed for the elements: C, H, O, N, P and S as follows.

Table 4: Amino acids (AA) with P and S as key ions and nucleo-bases.

	Amino acid	**Ions**	**Formula**	$\mathcal{M}$**(AA)**	**Key/master ion ratio**
SEP (S)	**Phosphoserine**	P^+	$C_3H_8NO_6P$	185.073	1/18
TPO (T)	**Phosphothreonine**	P^+	$C_4H_{10}NO_6P$	199.10	1/21
PTR (Y)	**O-phosphotyrosine**	P^+	$C_9H_{12}NO_6P$	261.17	1/27
CSO (C)	**S-hydroxycysteine**	S^+	$C_3H_7NO_3S$	**137.16**	1/14
HIP (H)	**Cysteine**	S^+	$C_3H_7NO_2S$	121.16	1/13
TAU (J)	**Taurine**	S^+	$C_2H_7NO_3S$	125.15	1/13
	Nucleo-bases				
A	**Adenine**	C^+, N^+, O^+	$C_5H_5N_5$	135.1267	-
T	**Thymine**	C^+, N^+, O^+	$C_5H_6N_2O_2$	126.04	-
C	**Cytosine**	C^+, N^+, O^+	$C_4H_5N_3O$	111.102	-
G	**Guanine**	C^+, N^+, O^+	$C_5H_5N_5O$	151.1261	-
U	**Uracil**	C^+, N^+, O^+	$C_4H_4N_2O_2$	112.0867	-

The **carbon** peaks allow a pre-evaluation of the virus molecular weight on the basis of the signal integration, the calculation of the mass of carbon in the virus and evaluation the virus mass from a standard virus molecular formula ($C_\chi H_\eta O_\omega N_\nu P_\pi S_\sigma$). A pre-identification may be derived following the classification proposed by Matthews (1975)[21]. For 59 different viruses, when the amount of nucleic acid in the particle is related either to the dry weight of the particle or to the particle volume, two classes of virus groups emerge - those with enveloped or those with geometrical particles.

Now let us examine the chemical association of the major and key ions in the virus phases.

Viral **oxygen** is linked to acidic, alcoholic, ketonic groups of bio compound but first to virus **hydration** (water), to be linked with the density i.e. real virus density or weight and virus anhydrous density or weight.

Viral **nitrogen** is associated to basic groups of bio compounds, i.e. ATCG (DNA) or ATCU (RNA) and specific amino acids.

Viral **phosphorus** is due to phosphate acid groups of bio compounds, it should be possible to distinguish DNA from RNA viruses and also phosphor- serine, threonine and tyrosine rich proteins.

Viral **sulphur** is found for thiol, thio-ketone groups of bio compounds as well as cysteine, methionine and taurine rich proteins.

Knowing the fractions the viral formula $C_\chi H_\eta O_\omega N_\nu P_\pi S_\sigma$ may be deduced from the SV ICP-MS peaks and the virus molecular weight.

Viruses belonging to the family ***Coronaviridae*** consists of species that are first recognised for their specific morphology (TEM), see for example **Fig. 3**. The characterization of spike proteins from viruses is of course important for antiviral drug development e.g. Shanker, *et al*

(2020)[22]. For SARS-CoV-2 the viruse's functions are dictated by its RNA. ***Coronaviridae*** protein compositions have been analysed since several decades e.g. Hierholzer *et al* (1972)[23] for the coronavirus OC 43. The buoyant density in potassium tartrate of the virus was 1.15 g cm^{-3} and of the intact OC 43 virion was 1.18 g cm^{-3}. By analytical ultracentrifugation the corrected sedimentation coefficient of the OC 43 virion was determined and the **apparent molecular weight** (M(vir)) was calculated to be **(112 ± 5) x 10^6** Da. The human respiratory coronavirus OC43 was isotopically labelled with amino acids, glucosamine, and orthophosphate to analyze virion structural proteins as reported by Hogue & Brian (1986)[24]. Major protein species were resolved by electrophoresis and many of their properties were deduced from digestion studies using proteolytic enzymes.

The **first** virus investigated in this work, the **SARS-COV 2 virus** was chemically described recently by Popovic & Minceva (2020)[25]. RNA and protein data utilized in this work are given in Table 5. The number of protein copies per virion varies, even within a single species (Neuman *et al.*, 2011) [26]. For example, the number of spike protein trimers can vary between 50 and 100 per virion. The average number is 74 trimers, giving 74 × 3 = 222 spike proteins in total (Neuman *et al.* , 2006) [27]. Total number of atoms constituting the viruses is gained by the atom counting method. For each virus, the number of atoms is given for the entire virion (nucleocapsid + envelope) and the nucleocapsid. The last line presents the molar mass of entire virions, in Daltons.

Fig. 3: SARS-COV 2 structure showing spikes, membrane and RNA genome. Adapted from Olena (2020)[28]. Biochemical composition, see **Table 5.**

The empirical formula of RNA was taken to be the average RNA of all RNA viruses considered in the atom counting method $CH_{1.2316}O_{0.7610}N_{0.3967}P_{0.1050}$.
The protein composition was taken as the average viral protein composition of all viruses considered in the atom counting method $CH_{1.5692}O_{0.3085}N_{0.2708}S_{0.0061}$, lipid composition was represented by that of human lipids $CH_{1.9216}O_{0.1176}$ (Wang *et al.*, 1993) [29] and non-nucleic acid carbohydrate composition may be represented by the empirical formula of carbohydrates CH_2O.

Table 5: Components, chemical formula and masses of a **SARS-COV-2** virus. Genome: Sense: → , Bases: A T C U , POD: phosphate desoxyribose.

Component	**Formula**	**Mass (Da)**	**Subunit**	**Mass tot (Da)**
Nucleoprotein Total	$C_{1971}H_{3137}N_{607}O_{628}S_7$ $C_{4667328}H_{7428416}N_{1437376}O_{1487104}S_{16576}$	45,625	2368	108,040,000
Membrane protein Total	$C_{1165}H_{1823}N_{303}O_{301}S_8$ $C_{1379360}H_{2158432}N_{358752}O_{712768}S_{9472}$	25,146	1184	29,772,864
Spike protein Total	$C_{6336}H_{9770}N_{1656}O_{1894}S_{54}$ $C_{1406592}H_{2168940}N_{367632}O_{420468}S_{11988}$	141,175	222	31,340,850
Total Protein	$C_{7453280}H_{11755788}N_{2163760}O_{2620340}S_{38040}$	-	-	169,153,714
Genome	$\rightarrow A_a T_t C_c U_u$			
Genome total	$C_{2646720}H_{4804202}N_{161240}O_{260660}P_{65230}Na_{65230}$	46,514,892	1	*52,346,286*
Virus total	$C_{10100000}H_{16560000}N_{2325000}O_{2881000}P_{65230}S_{38040}Na_{65230}$		1 filled capsid	221,500,000

The **second** examined case is the ***Siphoviridae*** **bacteriophage T5** virus which morphological characteristics are depicted **Fig. 4** and chemical composition reported in Table 5. The huge

105 MDa DNA-filled viral particle mass was accurately measured using a nano-mechanical mass spectrometer as reported by Domingez-Medina (2018)[30]. DNA was taken to be the average DNA of all DNA viruses considered in the atom counting method $CH_{1.2555}O_{0.5840}N_{0.3796}P_{0.1022}$.

Fig. 4: Morphological characteristics of the *Siphoviridae* bacteriophage T5 virus, adapted from Domingez-Medina (2018). Biochemical composition, see **Table 6.**

Table 6: Components, chemical formula and masses of a ***siphoviridae*** **bacteriophage T5**. Genome: Sense: →, antisense: ←, Bases: A T C G , POD: Na phosphate desoxyribose.

Component	Formula	Mass (Da)	Subunit	Mass tot (Da)
Head protein pb8	$C_{1466}H_{2349}N_{391}O_{445}S_5$	32,892	775	25,491,633
Total	$C_{1136150}H_{1820475}N_{303025}O_{344875}S_{3875}$			
Portal protein pb7	$C_{1948}H_{3099}N_{523}O_{601}S_{13}$	43,879	12	526,548
Total	$C_{23376}H_{37188}N_{6276}O_{7212}S_{156}$			
Empty capsid				26,018,181
Head completion protein p144	$C_{853}H_{1352}N_{224}O_{263}S_8$	19,210	12	230,521
Total	$C_{10236}H_{16224}N_{2688}O_{3156}S_{96}$			
Total proteins	$C_{1169762}H_{1873887}N_{311989}O_{355243}S_{4127}$			26,248,702
Genome bases	$\rightarrow A_{36051}T_{37888}C_{23473}G_{24388}$ $C_{20}H_{35}N_7O_8Na_2P_2$	650	121,750	79,137,500
	$\leftarrow A_{37888}T_{36051}C_{24388}G_{23473}$	*620*	*121,800*	*75,516,000*
Genome Elements	$\rightarrow$ $C_{585527}H_{609790}N_{438390}O_{123637}$			
	$\leftarrow$ $C_{584612}H_{609000}N_{452071}O_{119963}$			
	POD: $C_{1218000}H_{569000}O_{121800}P_{243600}Na_{243600}$			
Genome total	$C_{2388139}H_{29971390}N_{900461}O_{1905200}P_{243600}Na_{243600}$		1	
Virus total	$C_{3557901}H_{4871277}N_{1212450}O_{2260443}P_{243600}S_{4127}Na_{243600}$		1	105,386,202

The researchers measured hundreds of DNA-filled viruses and found that the normalised distribution of measured masses centred on 108.4 MDa. This value is slightly higher than the calculated molecular mass of 105.4 MDa, perhaps because of salt introduced during ionisation, or the degree of hydration.

Application of SV ICP-MS

The full calculation of a SV ICP MS may be estimated as follow:

1. establish the molecular formula $C_\chi H_\eta O_\omega N_\nu P_\pi S_\sigma$ of the virus
2. with Eq 1 and 2 derive the peak characteristics,
3. with Eq 3 derives the number of peak per time unit from the virus number concentration in the original sample.

Figure 5 shows the scan that can be recorded for the 2 virus types studied in this work.
The peak intensity recorded for ^{13}C, ^{15}N, ^{31}P, ^{32}S can be used to identify the virus, and the frequency in the scan is directly proportional to the virus concentration.

For the COV-2 virus, the molar ratio's are:

N/C = 0.230; P/C = 0.0065 and S/C = 0.00377.

For this RNA virus, the single rather short genome chain contributes to a small P/C ratio and a slightly reduced N/C ratio compared to the *siphoviridae* case treated below. The COV-2 is however known to be rather sulphur rich and the S/C ratio is larger here than for the bacteriophage T5 (DNA virus).

For the *siphoviridae* (DNA virus) the ratios are:

N/C = 0.313; P/C = 0.0684 and S/C = 0.0012.

Mass fractions are often used in human body composition research, for example the composition of an average adult is 21.0% C, 10.2% H, 63.7% O, 2.7% N, 0.7% P, 0.2% S and 1.6% other elements (Wang et al., 1993).
The human body molecular average ratio's are:

N/C = 0.11; P/C = 0.013 and S/C = 0.0036.

Fig. 5: Simulated SV ICP MS scan for analysis of Viruses.
a. 24 single SARS COV-2 viruses +2 counted as double
b. 16 single *siphoviridae* bacteriophage T5 viruses +1 counted as double.
Conditions: recording time 2 s, Δt: 10 ms, η_C : $2x10^{-2}$, η_A: $^{13}C^+$: 1.10%, $^{15}N^+$: 0.366%, $^{31}P^+$: 100%, $^{32}S^+$: 95%, other conditions see Table 1. Readings: **a.** at 0.26 s and 1.95 s: aggregates of 2 viruses, 1.38 bio-fragment e.g. cellulose nano particle, **b**. at 0.42 s: aggregate of 2 viruses, for **a.** & **b.** the $^{13}C^+$ background is due to residual DOC and traces of CO_2, the $^{15}N^+$ background is due to residual dissolved N_2 in solution and traces of N in DOC.

Recommendations

The single virus analysis challenge is to discriminate the C and N ICP-MS peaks from the virus from the C and N signal backgrounds. Clearly reduction of both background signals is possible working in a helium glove box (also required to avoid viral contamination) and using argon for the plasma torch with at least a seven 9 quality argon at least during sample injection. The argument C and N analysis by ICPMS is not possible is wrong this is due to the air contamination because ICP-MS analysis is traditionally carried out in atmospheric conditions. Actually C and N analyses are possible e.g. Riisom, *et al* (2018)[31]. Reduction of both C (CO_2 and TOC) and N (N_2) in the samples and ultra pure water used for dilution is mandatory. Interferences (see Table 2) need to be carefully assessed and reduced if any. Carbonates, bicarbonates and carbon dioxide as well as all soluble organic materials must be eliminated for carbon SV ICP-MS analysis. For nitrogen SV ICP-MS, nitrate, nitrite and ammonium as well as organic nitrogen compounds must also be eliminated. As an example using the reciprocal of Eq. 2 the signal s_{15N+} for a 1 ppb N_2 argon - N free sample would be 300 counts for a 1μs Δt (slot time).

For phosphorus and sulphur, all interferences (see Table 3) need to be carefully assessed and reduced if any. A Pt cone is required to avoid any interference from $^{62}Ni^{2+}$ (η_A: 3.6%) with $^{31}P^+$ and $^{64}Ni^{2+}$ (η_A: 0.926%) with $^{32}S^+$. Both could be recorded with the classical nickel cone. Phosphates, phosphites and phosphine as well as organophosphorus (e.g. phosphinites and phosphonites) compounds must be eliminated prior phosphorus SV ICP-MS analysis. Sulphate, sulphites and sulphides as well as sulphurous organic compounds must be absent from the sample prior SV ICP-MS analysis.

The volume of the torch is an issue as well as the size of the cone hole as well as the thermo-hydraulic properties of the plasma (plasma, power source, temperature …). Optimal argon flows, nebulisation and dilution in ultrapure water are a must. Here, the work is carried out for 100 nm viruses using CNPS signals. Interest for other labeling elements such as Se or Na, K, Mg, Ca, Zn and also for smaller viruses should be mentioned. This requires however an improvement of the sensibility e.g. from the pg to the fg level.

To avoid interferences the use of sector field ICP-MS is suggested e.g. Jakubowski *et al* (1998)[32]. Work with TOF MS is difficult, quadrupole MSs are better but sector field MSs are strongly recommended to avoid interferences.

Future work concerns the comparison of SV ICP MS scans as calculated for a larger series of viruses with molecular formula $C_\chi H_\eta O_\omega N_\nu P_\pi S_\sigma$ as those given by Popovic & Minceva (2020)[33], for both type (RNA and DNA viruses) and for sizes going from ~20 (if possible) to ~200 nm.

4. Conclusions

This paper is an attempt to review and summarize the different approaches applicable in relation to the detectability in single virus ICP-MS analysis, and highlight the peculiarities of this topic. Interferences are analysed and discussed pointing out the need of SF-ICP-MS.

The analysis of single viruses by SV ICP-MS is possible routinely, recording MS peaks in time scan for given masses and detecting say 2 to 500 viruses in 20 s. The time required for virus counting by SV ICP MS is several thousand time faster than by the other techniques e.g. electron microscopy. Their identification is based on the carbon peak intensity (e.g. $^{13}C^{+}$) which based on the virus molecular weight or mass and the ratio of other master ions (N as surrogate for nucleo-bases and amino acids) and key ions (P as leading element for phosphate from the nucleo-chains, and S for thiol groups) peaks. A virus classification based on the N/C, P/C and S/C molecular ratios is suggested.

Acknowledgements

Acknowledgements are due to Dr Bodo Hattendorf from ETHZ for the constructive discussion we had to optimise the recommendations.

References

[1] C. Degueldre, P.-Y. Favarger, *Colloid analysis by single particle inductively coupled plasma-mass spectroscopy: a feasibility study*, Colloids and Surfaces A, 217 (2003) 137-142 . doi:10.016/S0927-7757(02)00568-X.

[2] C. Degueldre, P. -Y. Favarger,S. Wold, *Gold colloid analysis by inductively coupled plasma-mass spectrometry in a single particle mode*, Analytica Chimica Acta, 555 (2006) 263-268 . doi.org/10.1016/j.aca.2005.09.021.

[3] C. Degueldre, P.-Y. Favarger, C. Bitea, *Zirconia colloid analysis by single particle inductively coupled plasma–mass spectrometry*, Analytica Chimica Acta, 518 (2004) 137-142 . doi:101016/jaca200404015.

[4] C Degueldre, P.-Y Favarger, *Thorium colloid analysis by single particle inductively coupled plasma-mass spectrometry*, Talanta, 62 (2004) 1051-1054. doi:10.016/j.talanta.2003.10.016.

[5] C Degueldre, P.-Y Favarger, R. Rosé, S. Wold, *Uranium colloid analysis by single particle inductively coupled plasma-mass spectrometry*, Talanta, 68 (2006) 623-628. doi: 10.1016/j.talanta.2005.05.006.

[6] J. Koch, D. Günther, *Laser Ablation Inductively Coupled Plasma Mass Spectrometry*, Encyclopedia of Spectroscopy and Spectrometry (Third Edition), (2017) 526-532.

[7] Ling-Na Zheng, Meng Wang, Bing Wang, Wei-Yue Feng, *Determination of quantum dots in single cells by inductively coupled plasma mass spectrometry*, Talanta, 116 (2013) 782-787. doi: 10.1016/j.talanta.2013.07.075

[8] M. Corte-Rodríguez, R. Álvarez-Fernández, P. García-Cancela, J. Bettmer, *Single cell ICP-MS using on line sample introduction systems: Current developments and remaining challenge*s, TrAC Trends in Analytical Chemistry, 132 (2020) 116042.

[9] R. S. Amais, G. L. Donati, M. A.Zezzi Arruda, *ICP-MS and trace element analysis as tools for better understanding medical conditions*, TrAC Trends in Analytical Chemistry, 133 (2020) 116094

[10] E. V. Shun'ko, D. E. Stevenson, V. S. Belkin, *Inductively Coupling Plasma Reactor With Plasma Electron Energy Controllable in the Range From ~6 to ~100 eV*. IEEE Transactions on Plasma Science. 42 (2014) 774–785.

[11] E. T. Luong, R.S Houk, *Determination of carbon isotope ratios in amino acids, proteins, and oligosaccharides by inductively coupled plasma-mass spectrometry*, J. Am. Soc. Mass Spectrom., 14 (2003) 295-301. doi:10.1016/S1044-0305(03)00003-5.

[12] J.G. Martínez-Sierra, O.G. San Blas, J.M.Marchante Gayón, J.I. García Alonso, *Sulfur analysis by inductively coupled plasma-mass spectrometry: A review*, Spectrochim. Acta B, (2015) 35-52. doi: 10.1016/j.sab.2015.03.016.

[13] S. Faßbender, K. Rodiouchkina, F. Vanhaecke, B. Meermann, *Method development for on-line species-specific sulfur isotopic analysis by means of capillary electrophoresis/multicollector ICP-mass spectrometry*, Anal. Bioanal. Chem., 412 (2020) 5637–5646. doi.org/10.1007/s00216-020-02781-8

[14] F. Laborda, A. C. Gimenez-Ingalaturre, E. Bolea, J. R. Castillo, *About detectability and limits of detection in single particle inductively coupled plasma mass spectrometry*, Spectrochim. Acta B. 169 (2020) 105883. doi: 10.1016/j.sab.2020.105883

[15] L. A. Rush, C. E. Mackenzie, M. Liezers, A. M. Duffin, *Collisional dampening for improved quantification in single particle inductively coupled plasma mass spectrometry*, Talanta 189 (2018) 268-273. doi: 10.1016/j.talanta.2018.06.071.
.

[16] M. Loula, A. Kaňa, O. Mestek, *Non-spectral interferences in single-particle ICP-MS analysis: An underestimated phenomenon*, Talanta, 202 (2019) 565-571. doi: 10.1016/j.talanta.2019.04.073.

[17] H. Vanhoe, J. Goossens, L. Moens, F.J. Dams, *Spectral and non-spectral interferences in inductively-coupled plasma mass-spectrometry***,** Microchim. Acta, 119 (1995) 277-286. doi: 10.1007/BF01244007.

[18] P. Kralj, M. Veber, *Investigations into nonspectroscopic effects of organic compounds in inductively coupled plasma mass spectrometry*, Acta Chim. Slov., 50 (2003) 633-644. doi:

[19] M. Witzler, F. Küllmer, K. Günther, *Validating a single-particle ICP-MS method to measure nanoparticles in human whole blood for nanotoxicology*, Anal. Lett., 51 (2018) 587-599. doi: 10.1080/00032719.2017.1327538.

[20] Y. Cao, J. Feng, L. Tang, Ch. Yu, G. Mo, B. Deng, *A highly efficient introduction system for single cell- ICP-MS and its application to detection of copper in single human red blood cells*, Talanta, 206 (2020) 120174. https://doi.org/10.1016/j.talanta.2019.120174

[21] R. E. F. Matthews, *A Classification of Virus Groups Based on the Size of the Particle in Relation to Genome Size* J. Gen. Virol. 27 (I975) 135-149. doi: 10.1099/0022-1317-27-2-135.

[22] A. K. Shanker, D. Bhanu, A. Alluri,' S. Gupta, *Whole-genome sequence analysis and homology modelling of the main protease and non-structural protein 3 of SARS-CoV-2 reveal an aza-peptide and a lead inhibitor with possible antiviral properties*, New J. Chem. 44 (2020) 9202-9212 https://doi.org/10.1039/D0NJ00974A

[23] J.C. Hierholzer, E.L. Palmer, S.G. Whitfield, H.S. Kaye, W.R. Dowdle, *Protein composition of coronavirus OC 43*, Virology 48 (1972) 516-527. doi: 10.1016/0042-6822(72)90062-1.

[24] B. G. Hogue, D. A. Brian, *Structural proteins of human respiratory coronavirus OC43*, Virus Res., 5 (1986) 131-144 doi:

[25] M. Popovic, M. Minceva, *Thermodynamic insight into viral infections 2: empirical formulas, molecular compositions and thermodynamic properties of SARS, MERS and SARS-CoV-2 (COVID-19) viruses*, Heliyon, 6 (2020) e04943. doi: 10.1016/j.heliyon.2020.e04943.

[26] B.W. Neuman, G. Kiss, A.H. Kunding, D. Bhella, M.F. Baksh, S. Connelly, B. Droese, J.P. Klaus, S. Makino, S.G. Sawicki, S.G. Siddell, D.G. Stamou, I.A. Wilson, P. Kuhn, M.J. Buchmeier, *A structural analysis of M protein in coronavirus assembly and morphology*, J. Struct. Biol., 174 (2011) 11-22. doi: 1016/j.jsb.2010.11.021.

[27] B.W. Neuman, B.D. Adair, C. Yoshioka, J.D. Quispe, G. Orca, P. Kuhn, R.A. Milligan, M. Yeager, M.J. Buchmeier, *Supramolecular architecture of severe acute respiratory syndrome coronavirus revealed by electron cryomicroscopy*, J. Virol., 80 (2006) 7918-7928 doi: 10.1128/JVI.00645-06

[28] A. Olena, *Remsevisir works against coronaviruses in the lab*. The Scientist 20 Mar. (2020).

[29] Z.-m. Wang, R. Ma, R.N. Pierson, S.B. Heymsfield, *Five level model: reconstruction of body weight at atomic, molecular, cellular, and tissue-system levels from neutron activation analysis*, K.J. Ellis, J.D. Eastman (Eds.), Human Body Composition, Plenum Press, New York (1993), pp. 125-128.

[30] S. Domingez-Medina, S. Forstner, M. Deffrt, M. Sansa, A-K. Stark, M.A. Halim, E. Vernhes, M. Gely, G. Jourdan, T. Alava, P. Boulanger, Ch. Masselon, S. Hentz, *Neutral mass spectrometry of virus capsids above 100 megadaltons with nanomechanical resonators*, Science 362 (2018) 918-922. doi: 10.1126/science.aat6457

[31] M. Riisom, B. Gammelgaard, I.H. Lambert, S. Stürup, *Development and validation of an ICP-MS method for quantification of total carbon and platinum in cell sample and comparison of open vessel and microwave assisted acid digestion methods*, J. Pharma. Biomed. Anal., 158 (2018) 144-150. doi: 10.1016/j.jpba.2018.05.038.

[32] N. Jakubowski, L. Moens, F. Vanhoecke, Sector field mass spectrometer in ICP-MS, Spectrochim. Acta B 53 (1998) 1739-1763. doi: 10.1016/S0584-8547

[33] M. Popovic, M. Minceva, *Thermodynamic insight into viral infections: do viruses in a lytic cycle hijack cell metabolism due to their Gibbs energy?*, Heliyon, 6 (2020) e03933. doi: 10.1016/j.heliyon.2020.e03933